International Journal of Recent Engineering Science
ISSN: 2349-7157/ https://doi.org/10.14445/23497157/IJRES-V13I1P101

Volume 13 Issue 1, 1-37, Jan-Feb 2026

Original Article

Observing Pre-Crystalline and Post-Crystalline Phase Transitions of 6OCB and 10OCB Liquid Crystals with 5 °C/min Ramp Rate Using DSC

Morgan Tiro[1], Dipti Sharma[2]

[1,2]*Emmanuel College, Boston, MA, USA.*

Received: 02 December 2025 Revised: 05 January 2026 Accepted: 22 January 2026 Published: 11 February 2026

Abstract - *This paper focuses on the unique behavior of 6OCB and 10OCB Liquid Crystals (LC) compared to 8OCB liquid crystal from the n-octyloxycyanobiphenyl (nOCB) thermotropic LC family. Three LCs from nOCB, 6OCB, 8OCB, and 10OCB were studied using the Differential Scanning Calorimetric (DSC) technique at a 5 °C/min ramp rate for heating and cooling. The DSC data was then analyzed in detail using Logger Pro. It is found that 6OCB is the youngest and lightest member of nOCB and shows a new state of pre-crystalline on heating, whereas 10OCB is the oldest and heaviest member of nOCB that shows a new state of post-crystalline on heating, when compared with 8OCB LC, whereas 8OCB shows nothing like that. These two new states make these LCs, 6OCB and 10OCB, very interesting material for research, showing bigger transition peaks, remaining in their distinct phases for a longer time, and having higher thermal energy occurring in these LCs. These novel states of matter make these LCs important in the research and application field of LCs. These unique states of 6OCB and 10OCB are explained with a predicted model of molecular alignment with the existence of a partially crystalline state as the Pre-Crystalline state in 6OCB, as it has the smallest tail size. At the same time, two energy levels are predicted in 10OCB LC: Crystalline and Post-Crystalline states, as it has the largest tail in its molecular structure. The presence of these unique states in 6OCB and 10OCB makes them more stable with wide and longer transition peaks, and can be useful considering them in Smart devices where a wide temperature range is required to manufacture them as Liquid Crystal Display devices (LCDs) or Smart watches or Smart Laptops.*

Keywords - *Liquid Crystals (LC), Differential Scanning Calorimetry (DSC), Specific heat capacity, Thermotropic, 6OCB, 8OCB, 10OCB, Crystalline, Smectic A, Nematic, Temperature, Heat flow, Phase change.*

1. Introduction

Liquid Crystals (LCs) are the materials that show multiple states of matter from Solid to Liquid, not just two, as Solid and Liquid. LCs differ from liquids and solids, as they combine both the properties described by liquids and solids. In a typical liquid, molecules are randomly arranged and move freely, while in solids, molecules are tightly packed in an ordered structure.

The unique nature of LCs allows them to manifest interesting optical, electrical, and medical properties.[1] The orientation of liquid crystals can easily be changed with temperature, and this is observed with heating and cooling them with Differential Scanning Calorimetry. LCs are known to absorb thermal energy as well as show endothermic peaks in heating, as seen in phase change transitions, but when cooled, they show release of heat as exothermic peaks.[2]

LCs can be divided into three main categories: lyotropic, metallotropic, and thermotropic LCs. Lyotropic LCs consist of organic molecules as well as some minerals, and show phase change transitions as a coupled function of the concentration of molecules in a solvent and temperature. Metallotropic LCs consist of both inorganic and organic molecules, and their phase change transition is dependent on the composition ratio of inorganic to organic molecules. Thermotropic LCs consist mostly of organic molecules and show phase change transitions into LCs as temperature is altered.[1] In this paper, we specifically examine the properties and behaviors of three thermotropic LCs in the nOCB family.

LCs have been drawing scientists' and researchers' attention for decades. LCs can be observed in distinct states, each differing in how their molecules are oriented or arranged. These phases include crystalline, smectic A or smectic C, nematic, and finally the isotropic phase. The crystalline state is the most ordered and resembles the arrangement of molecules in solids. Molecules in crystalline LCs are arranged in a positional and orientational order, and are tightly packed

in a three-dimensional lattice. The smectic A phase of LCs holds a partially ordered orientation of molecules with distinct layers in the lattice. The positional order of the molecules in the one-dimensional layers may change, but the orientational order remains, with molecules in the same plane. In the nematic phase of LCs, molecules are oriented in the same general direction but are no longer arranged in layers, allowing them to move freely and resembling a liquid. In the isotropic phase, molecules are fully disordered, resembling a liquid. There is no positional or orientational order, as molecules are randomly arranged and move freely.[3] These phase changes can be observed when heating and cooling LCs and occur in the order described during heating, and in the reverse order during cooling.[4]

LCs can be observed in many applications of everyday life. They have transformed our technology and are found in devices we use every day, such as smart technologies like cell phones, televisions, and computers. [3] or medicals or healthcare. We can even see thermotropic chiral LCs being used in the world for measuring temperature in thermometers. These types of crystals showcase a change in pitch with temperature, allowing them to serve as liquid crystal thermometers.[5] As the change in temperature is measured, the pitch is altered, causing the LC to reflect a color change, indicating temperature changes. These types of thermometers are usually used as pool thermometers or for infants. We can also see LC being used in fashion trends such as mood rings, where the color change is a response to a change in temperature, reflecting different colors based on body heat.[3]

The interest of this research is in thermotropic LCs, especially the nOCB category, belonging to a family of cyanobiphenyls. The nOCB is called alkylOxyCyanobiphenyl LCs. The most important thing in this family is the presence of an Oxygen atom. Because of the Oxygen atom, the nOCB LC behaves differently from other members of thermotropic LCs, for example, AlkylCyanobiphenyl (nCB), the LC family that does not have Oxygen. These types of studies on the nCB family of LCs can be seen here. [6-8] Because of Oxygen, the nOCB shows the presence of several types of states of matter between solid and liquid states, and sometimes, some members also show the absence of some states of matter, but then show some uniqueness. The nOCB is heavier than nCB as it has one Oxygen atom in it.

The nCB has been studied widely, but the nOCB has not been studied much. The novelty of nOCB, especially 6OCB and 10OCB, makes these LCs more important for research, as there is almost no literature on detailed studies of these LCs. The goal in selecting the nOCB family of LC is to examine the behaviors and properties of selected members of this family in response to heating and cooling them using an instrument called Differential Scanning Calorimetry (DSC). The members of the nOCB family that will be studied in this paper are 6OCB, 8OCB, and 10OCB. These members were selected to focus on the novelty of the features obtained in 6OCB and 10OCB in comparison to 8OCB. This research was conducted to examine how the molecular size of LC in the nOCB family may affect the phase change behavior, stability, and transition temperatures. The Novelty of the existence of new states of matter in 6OCB and 10OCB makes this research highly important in the area of LCs and their applications.

2. Theory, Materials, Structure, Phases, and Methods

2.1. Theory: Thermodynamics of LCs

This research focuses on the thermodynamics of LCs. The details of the theory used in this study can be seen below, following Physics and especially the branch of Physics called thermodynamics. The heat in Joules (Q) is dependent on the mass of a substance in grams (m), the specific heat capacity of the substance in J/g*°C (Cp), and the temperature change in °C (dT), as expressed in Equation 1. Rather than measuring total heat, DSC measures heat flow in Watts (dQ/dt) [7], and is related to the ramp rate (dT/dt), as seen in Equation 2. Specific heat capacity (Cp) can be determined by Equation 2, as seen in Equation 3.

$$Q = m*Cp*dT \quad (1)$$

$$dQ/dt = m*Cp*dT/dt \quad (2)$$

$$Cp = (dQ/dt)/[m*(dT/dt)] \quad (3)$$

The heat flow (HF) of LCs can be seen as a function of the rate of heat transfer with respect to time (dQ/dt) as HF = Heat Flow = (dQ/dt). The ramp rate used for this study is 5 °C/min and can be written as Rate = dT/dt = 5 °C/min = 5 °C/60 s = 1/12 °C/s. Specific heat capacity (Cp) can be related to HF by multiplying by 12 as Cp = HF*12.

2.2. Materials: 6OCB, 8OCB and 10OCB

Three thermotropic LCs from the family of nOCB were taken as HexylOxyCyanobiphenyl (6OCB), OctylOxyCyanobiphenyl (8OCB), and DecylOxyCyanobiphenyl (10OCB) for this study. All three are thermotropic liquid crystals whose molecular arrangement and alignment change with temperature change. They have an oxygen molecule connected between their tail and the body of the molecule. The “n” is the C-H chain and makes the tail of the molecule, and “CB” is the Cyanobiphyl group that makes the body of the molecule, and “O” is the oxygen that is connected in between them for all three molecules. The 6OCB is the “youngest” and smallest member of the three samples chosen for the study. The 10OCB is the “oldest” and largest of the three LCs in the study, and the 8OCB is considered a normal member because it falls between the 6OCB and 10OCB LCs. Usually, the 8OCB shows three phase transitions during heating and cooling, known as the solid-to-liquid states of Crystallization, Smectic A, and Nematic; however, it has

four states: Crystalline, Smectic A, Nematic, and Isotropic. The details of nOCB, 8OCB, and nCB LCs can be seen in these published articles. [9-12]

2.3. Molecular Structure

The molecular structures of the nOCB family of liquid crystals contain two benzene rings, one oxygen atom, a cyano group, and a tail with "n" number of C-H groups. OctylOxyCyanobiphenyl (8OCB), seen in Figures 1 and 2, is known to be a thermotropic LC found within the nOCB LC family. As seen in the 2D and 3D molecular structures of 8OCB, the molecule contains an Oxygen atom, two benzene rings, a cyano group, and the tail containing eight C-H groups.[7] The 8OCB LC's molecular weight is found to be 307.43 g/mol [8]. Seen in Figures 3 and 4 of the 2D and 3D models of HexylOxyCyanobiphenyl (6OCB), this molecule also belongs to the nOCB family, and is a smaller member, containing an Oxygen atom, two benzene rings, a cyano group, and the tail containing six C-H groups. The molecular weight of 6OCB is 279.38 g/mol. Finally, as seen in Figures 5 and 6 of the 2D and 3D molecular structures of DecylOxyCyanobiphenyl (10OCB), this molecule belongs to the nOCB family as well, and is a larger member, containing an Oxygen atom, two benzene rings, a cyano group, and the tail containing ten C-H groups. The molecular weight of 10OCB is 335.59 g/mol.

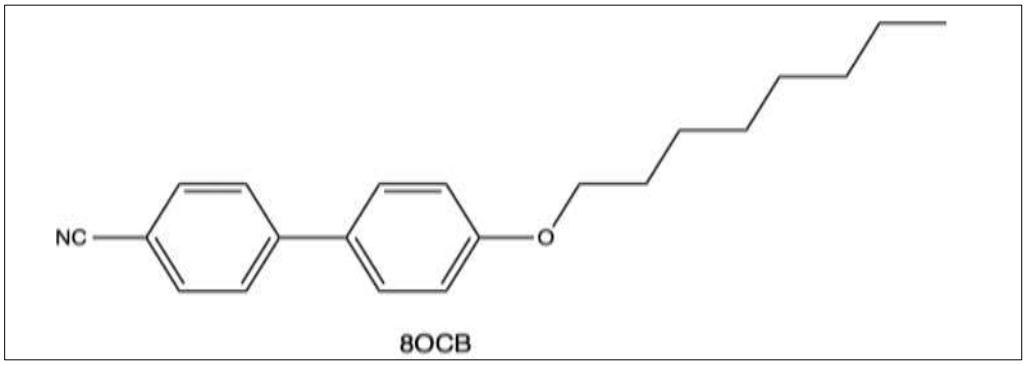

Fig. 1 Molecular Structure of 8OCB Liquid Crystal

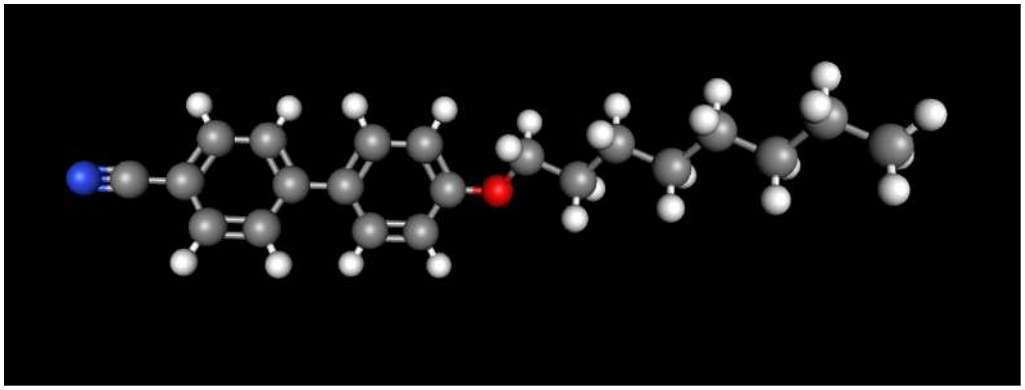

Fig. 2 3D Molecular Structure of 8OCB Liquid Crystal

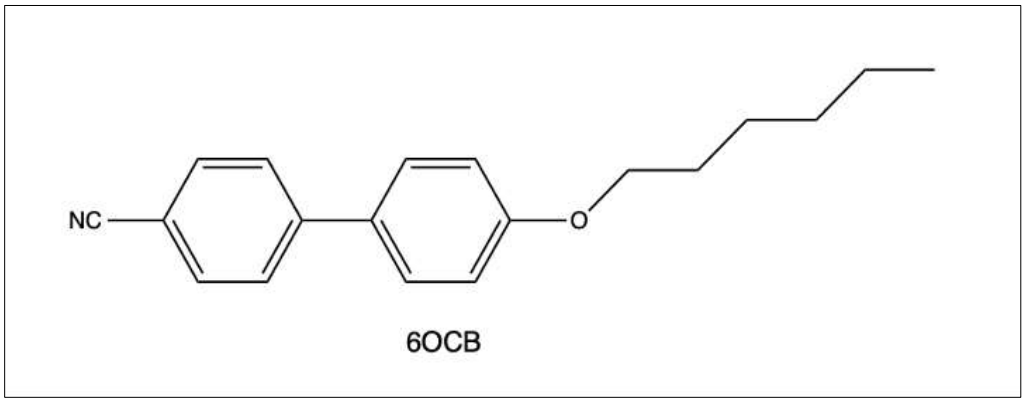

Fig. 3 Molecular Structure of 6OCB Liquid Crystal

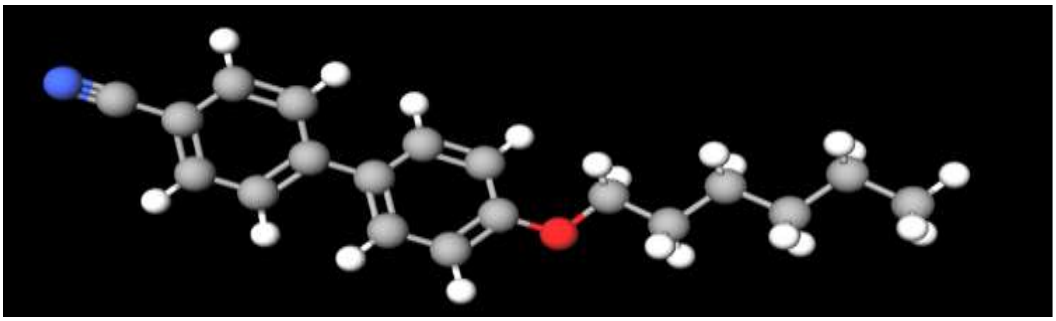

Fig. 4 3D Molecular Structure of 6OCB Liquid Crystal

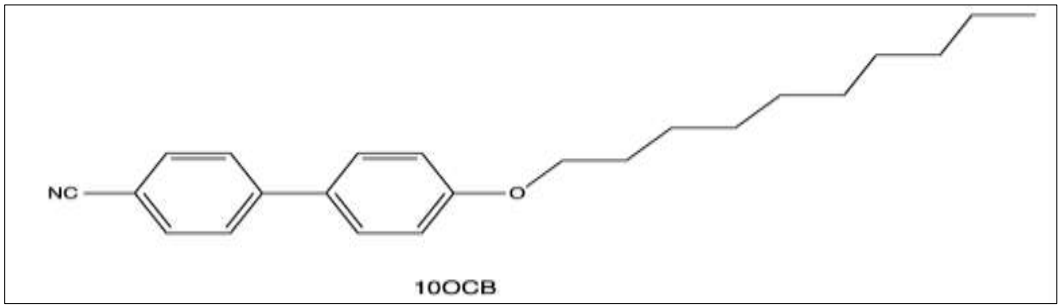

Fig. 5 Molecular Structure of 10OCB Liquid Crystal

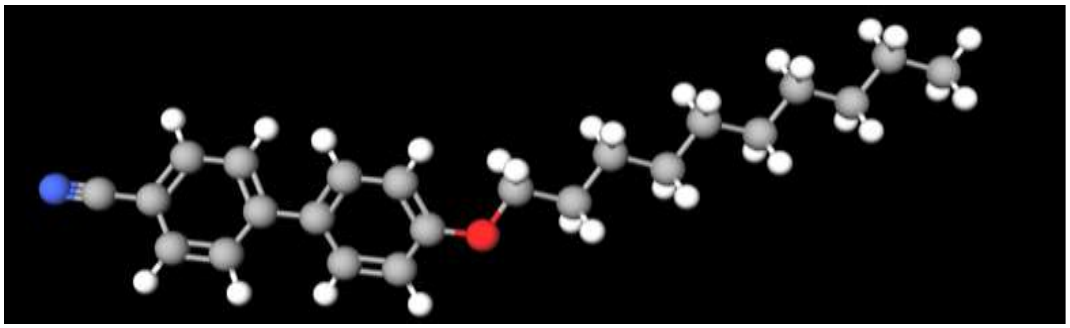

Fig. 6 3D Molecular Structure of 10OCB Liquid Crystal

2.4. Molecular Alignment and Phases

The 8OCB LC is considered a typical member of the nOCB family. This 8OCB LC shows four states of matter from Solid to Liquid states. These states are called the phases of the LC. These four phases are Crystalline, Smectic A, Nematic, and Isotropic. Where Crystalline is considered a complete solid state, and Isotropic is considered a complete liquid state. The rest of the phases are between the Solid and Liquid states. Since this LC molecule is large in size, it can be seen to look like a rod. The four states of 8OCB with its molecular arrangement and alignment in each phase can be seen in Figure 7.

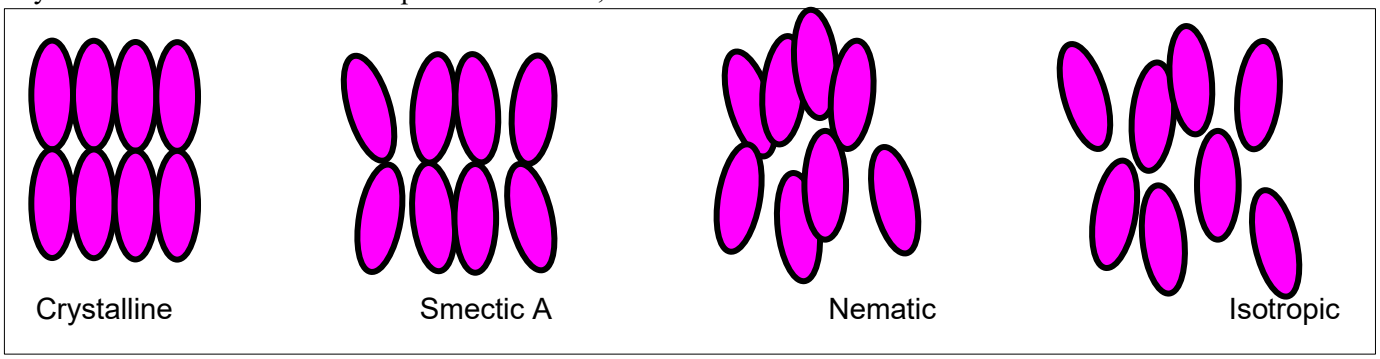

Fig. 7 Typical Molecular arrangement of 8OCB Liquid Crystal

The 8OCB has been studied by other authors, and its details can be seen here. [7-9] The main goal in this paper is to find the uniqueness of the younger and older members of the family of nOCB compared with 8OCB, considering 8OCB as a typical member of the nOCB family. When 6OCB and 10OCB were studied using DSC, it was found that there is something either missing or present in these LCs that 8OCB does not have. The goal is to find out what these properties are. Compared to the 8OCB molecular arrangement, the molecular arrangements of 6OCB and 10OCB are shown below as Figures 8 and 9, with a question mark present in these Figures to investigate what these phases are.

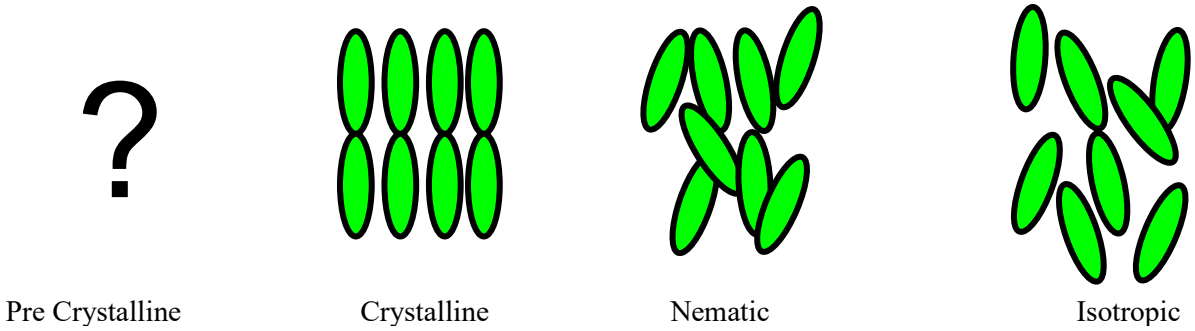

Fig. 8 Typical Molecular arrangement of 6OCB Liquid Crystal

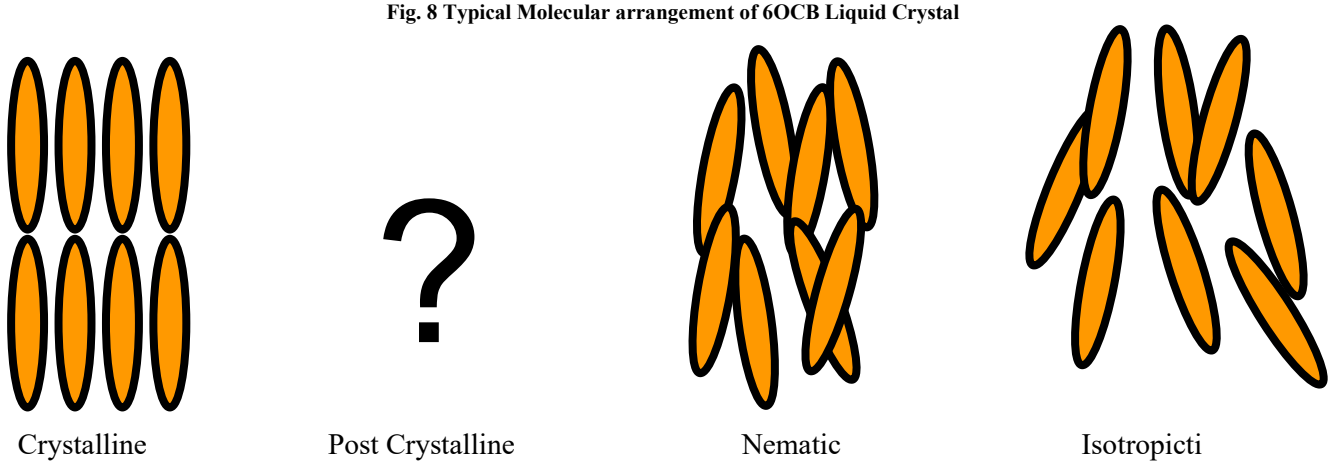

Fig. 9 Typical Molecular arrangement of 10OCB Liquid Crystal

2.5. Methods: DSC Technique

For this research, three different samples of nOCB were taken as 6OCB, 8OCB, and 10OCB. A small amount of each of them was placed in an aluminum cup and lid system and sealed. Then the sealed cup-lid with the sample was taken into the instrument called Differential Scanning Calorimetry, model 214 instrument, from the NETZSCH company at WPI chemistry and biochemistry department, Worcester, MA. All three samples were heated from -40 °C to 100 °C and then cooled back from 100 °C to -40 °C with a ramp rate of 5 °C/min for heating and cooling. The data produced by DSC was then collected from the DSC to show how heat flows in the sample with time and temperature. These data were then taken to Logger Pro for further detailed analysis of all three samples' thermal behavior. The thermal behavior of these samples was analyzed isothermally (when the temperature of the sample is changed and the corresponding heat flow is measured) and then computationally manipulated to explore the Specific Heat Capacity (Cp) of these samples. Some similar types of results are published with LCs, and DSC can be seen in these publications. [7-15].

2.5.1. Data and Results

A detailed study of 6OCB and 10OCB LCs was done using the DSC technique to see what unique behavior 6OCB and 10OCB show when compared with 8OCB LC. Data for all three LCs, 6OCB, 8OCB, and 10OCB, were obtained from DSC, and then a detailed analysis was performed using Logger Pro data analysis software for heating and cooling. These Figures 10-50 show the analysis of these samples.

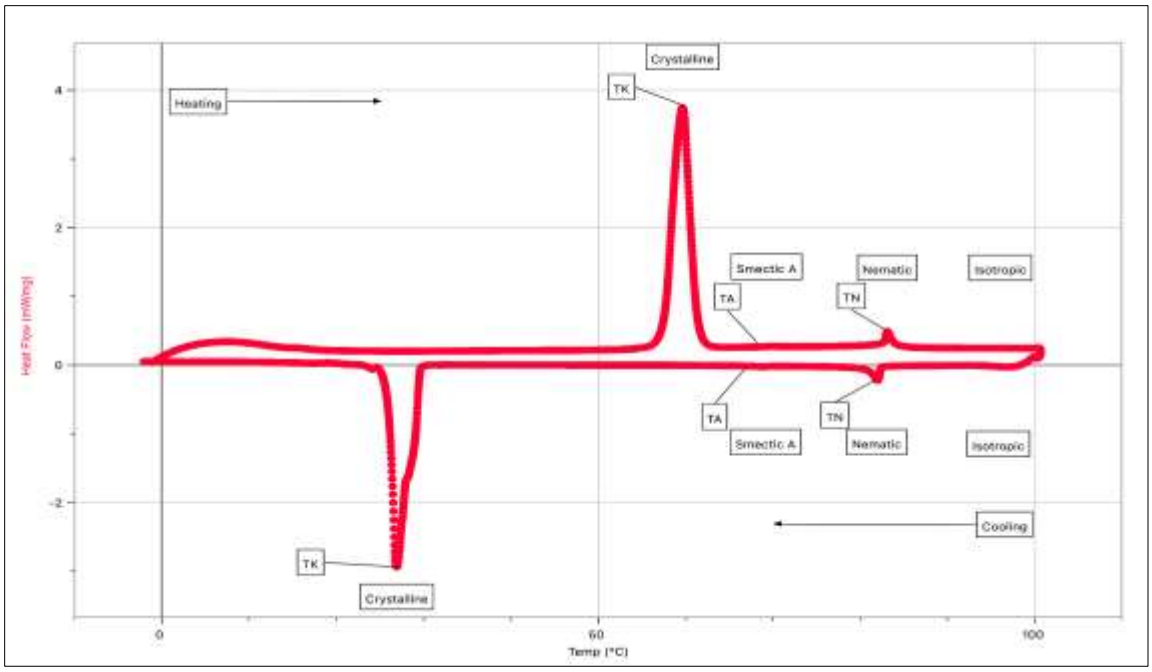

Fig. 10 Heat Flow (HF) vs Temperature (T) graph of 8OCB sample, heating and cooling

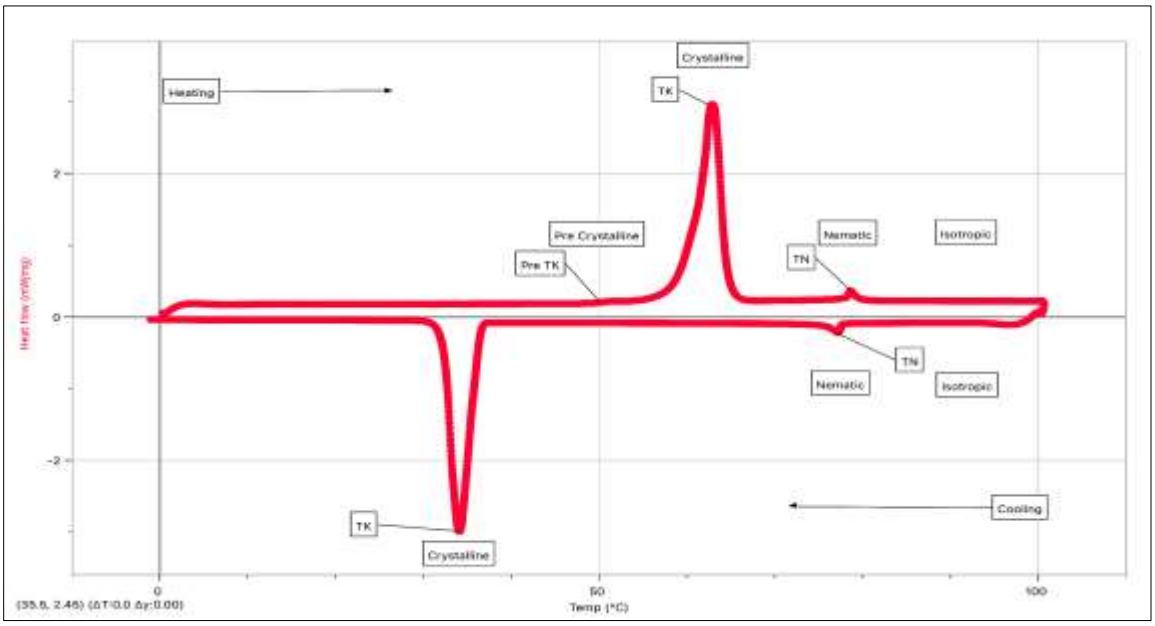

Fig. 11 Heat Flow (HF) vs Temperature (T) graph of 6OCB sample, heating and cooling

The 8OCB LC is a typical member of the nOCB family that is being researched. In Figure 10, the heat flow (HF) vs temperature graph can be seen for the heating and cooling of the sample in DSC.

The 8OCB is seen to present crystalline, smectic A, nematic, and isotropic phases in both heating and cooling. Peaks of each phase are labeled as follows: Crystalline = Tk, Smectic A = TA, Nematic = TN.

In Figure 11, the 6OCB LC can be viewed as a "younger" member of the nOCB family. In analyzing the 6OCB LC phase change transitions, a pre-crystalline, crystalline, nematic, and isotropic phase can be seen in heating. In cooling, a crystalline, nematic, and isotropic phase can be seen, but the pre-crystalline phase is no longer observed. No Smectic A phase is seen in the 6OCB display in either heating or cooling. Peaks of each phase are labeled as follows: Pre-Crystalline = Pre Tk, Crystalline = Tk, Nematic = TN.

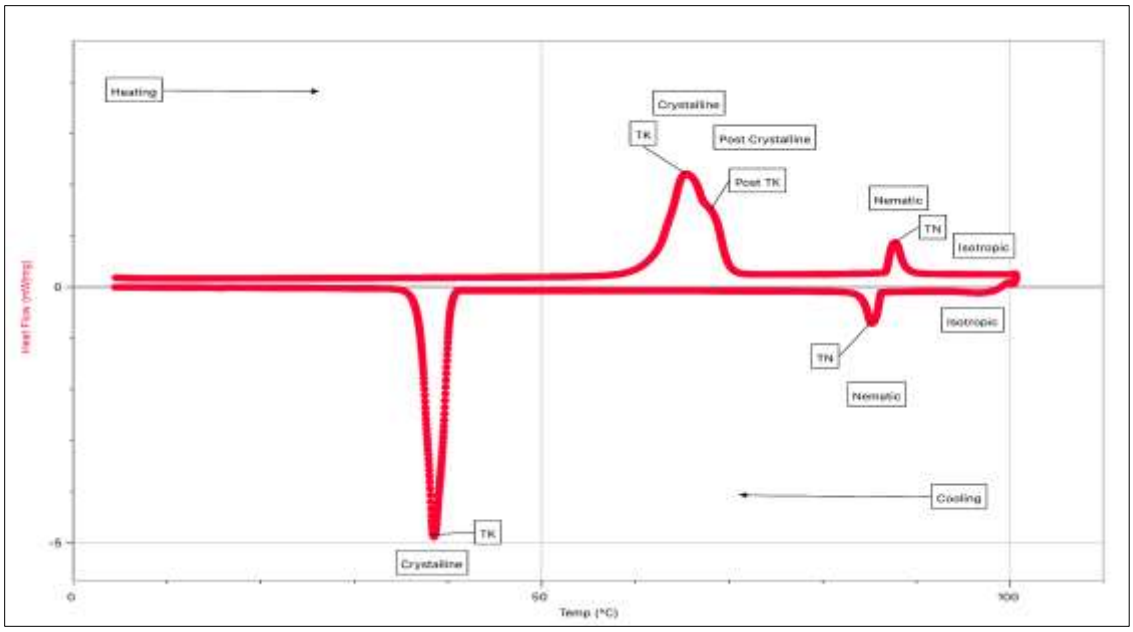

Fig. 12 Heat Flow (HF) vs Temperature (T) graph of 10OCB sample, heating and cooling

The 10OCB LC can be viewed as an "older" member of the nOCB family. In analyzing the 10OCB LC phase change transitions, a crystalline, post-crystalline, nematic, and isotropic phase can be seen in heating. In cooling, a crystalline, nematic, and isotropic phase can be seen, but the post-crystalline phase is no longer observed. No Smectic A phase is seen in the 10OCB display in either heating or cooling as well. Peaks of each phase are labeled as follows: Crystalline = Tk, Post-Crystalline = Post Tk, Nematic = TN.

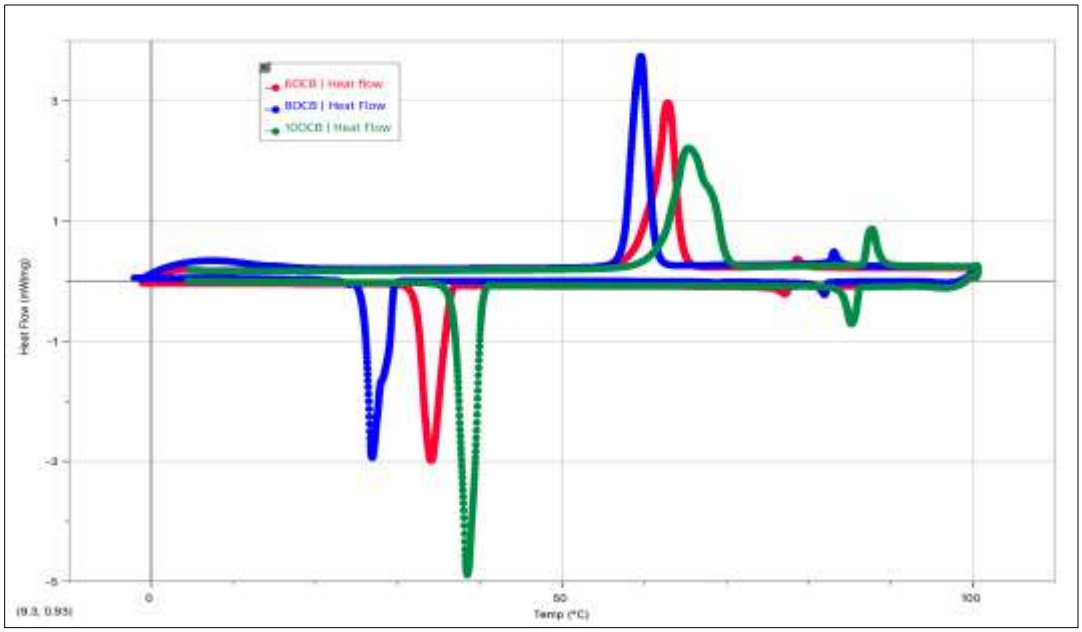

Fig. 13 Heat Flow (HF) vs Temperature (T) graph of all three LCs, 6OCB, 8OCB, and 10OCB samples, heating and cooling

During the heating and cooling of the samples, seen in Figures 10-13, each LC displays a distinct sequence of phase transitions. In heating, it can be observed that each sample exhibits the crystalline phase first. 6OCB shows a small and wide peak second, and 10OCB shows a much shorter and wider double peak last, when compared to 8OCB, which displays the crystalline peak first as a sharp, tall peak. Following the crystalline peaks, only 8OCB appears to display a Smectic A peak, as seen in Figure 38, zoomed in on this area. Nematic peaks can be seen next, with 6OCB first, 10OCB last,

and 8OCB second. The 6OCB sample exhibits the smallest nematic peak, 10OCB exhibits the largest nematic peak, and 8OCB shows an intermediate-sized nematic peak. In heating, it can be seen that there is a short temperature range between the crystalline peaks and the nematic peaks. Following nematic peaks, an isotropic phase can be seen for all three samples. In cooling the nOCB samples, nematic phases can be observed first after the isotropic phase. The 10OCB sample displays the nematic peak first, with a large peak, and 6OCB exhibits the smallest nematic peak last, while 8OCB again shows an intermediate-sized nematic peak between the 10OCB and 6OCB samples. A smectic A phase can also be observed in only the 8OCB sample, as seen in Figure 50, zoomed in on this area, after the nematic peaks. Once again, all three samples exhibit a crystalline phase as well in cooling, with 10OCB occurring first, displaying a large and sharp peak, followed by 6OCB next with a shorter and wider peak, and lastly 8OCB, displaying a short and wide double peak. In cooling, it can be seen that there is a much larger temperature range between the nematic and crystalline peaks.

Graphs were also made to examine the relationship of the Heat Flow (HF) vs time (min) for each of the three samples, and can be seen below.

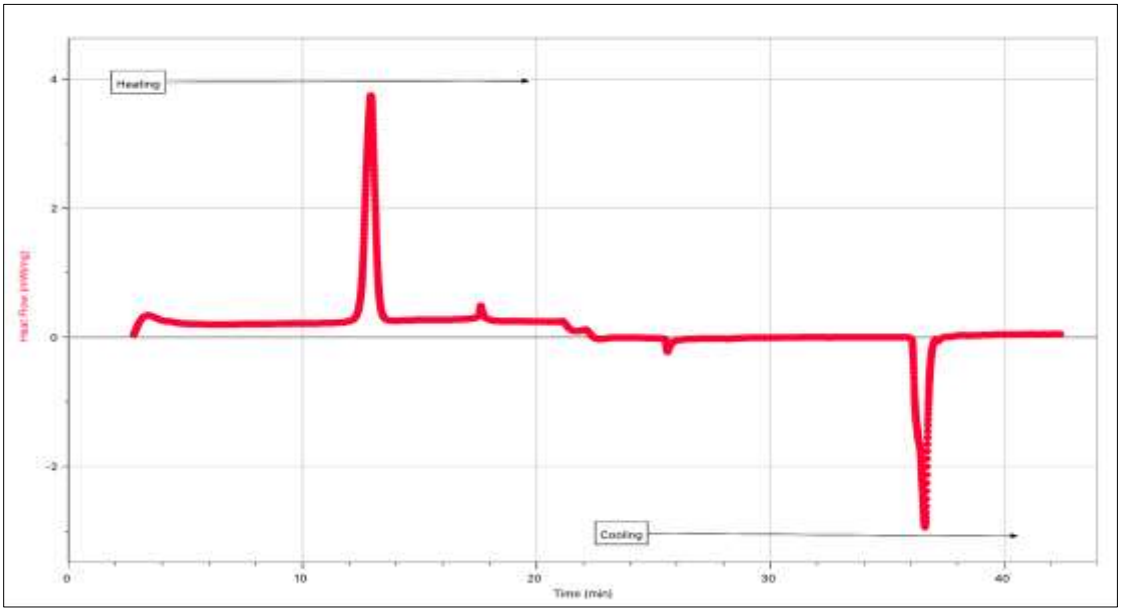

Fig. 14 Heat Flow (HF) vs Time (t) graph of 8OCB sample, heating and cooling.

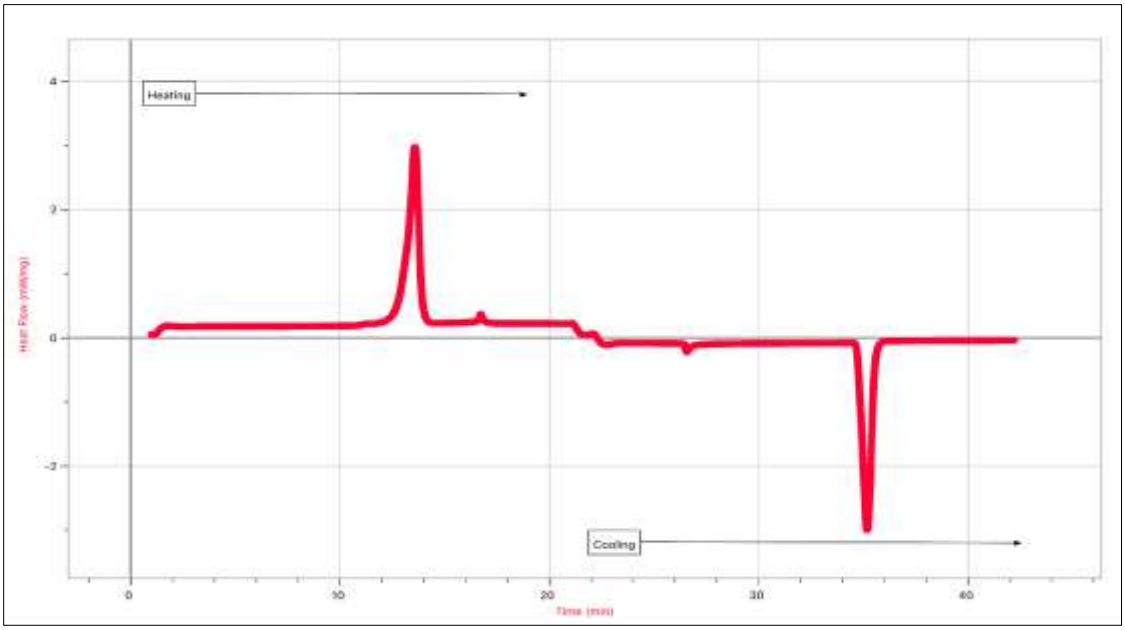

Fig. 15 Heat Flow (HF) vs Time (t) graph of 6OCB sample, heating and cooling.

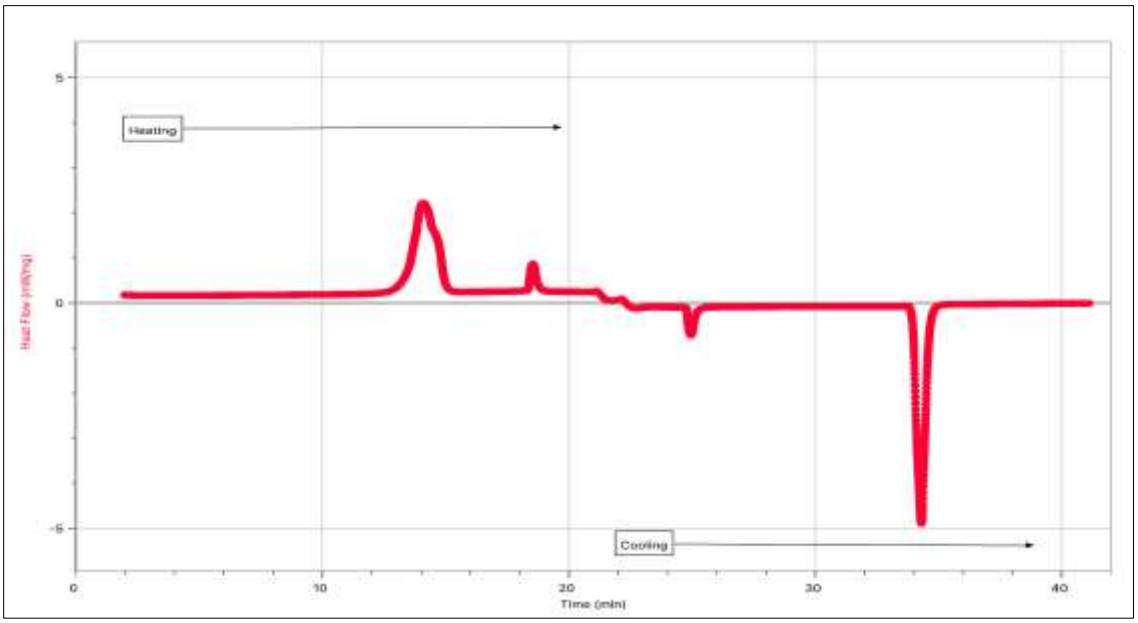

Fig. 16 Heat Flow (HF) vs Time (t) graph of 10OCB sample, heating and cooling.

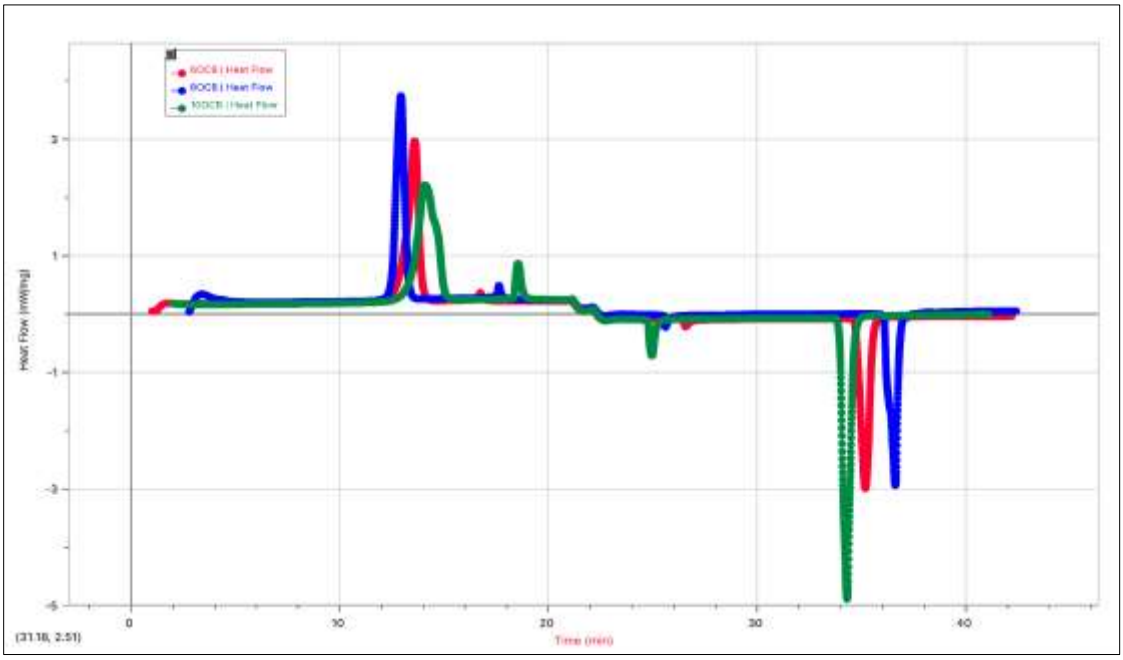

Fig. 17 Heat Flow (HF) vs Time (t) graph of all three samples, 6OCB, 8OCB, and 10OCB for heating and cooling.

In Figures 14-17, it can also be seen that during the heating and cooling of the samples, each LC displays a distinct sequence of phase transitions. The heating of all three samples can be observed until approximately 20 minutes, while the cooling of the samples occurs beyond 20 minutes. The pattern and order of peaks observed above follow the same pattern and order of peaks seen in Figure 13 of heat flow versus temperature. During the heating of the samples, it can be observed that each sample exhibits the crystalline phase first at approximately 12-16 minutes, with 8OCB appearing to display the crystalline peak first, followed by 6OCB, and finally 10OCB last. 6OCB shows a relatively small and wide crystalline peak, and 10OCB shows a much shorter and wider double peak, compared to 8OCB, which has a sharp, tall peak.

Once again, following the crystalline peaks, only 8OCB displays a smectic A peak, while 10OCB and 6OCB do not. Nematic peaks can be seen next between approximately 16-20 minutes, with 6OCB first, followed by 8OCB, then 10OCB. The 6OCB sample exhibits the smallest nematic peak, while

10OCB shows the largest nematic peak, compared to 8OCB, which shows an intermediate-sized nematic peak. In heating, it can now be seen that there is a short time range between the crystalline peaks and the nematic peaks. Following nematic peaks, an isotropic phase can be seen for all three samples. In cooling the nOCB samples after 20 minutes, nematic phases can be observed first after the isotropic phase, between approximately 24 and 28 minutes. The 10OCB sample displays the nematic peak first, with a large peak, and 6OCB shows the nematic peak last, with the smallest peak, compared to 8OCB, which shows an intermediate-sized peak. A smectic A phase can also, again, be observed in only the 8OCB sample after the nematic peaks. All three samples exhibit a crystalline phase during cooling between approximately 32-38 minutes, with 10OCB occurring first, displaying a large and sharp peak, followed by 6OCB, with a shorter and wider peak, and lastly 8OCB, displaying a short and wide double peak. In cooling, it can now be seen that there is a much larger time range between the nematic and crystalline peaks.

Table 1(a). Time of Peak of Transitions for Heating with 5 °C/min Ramp Rate.

Sample	t_pre (min)	t_k (min)	t_post (min)	T_Sm (min)	t_N (min)
6OCB	11.28	13.61			16.73
8OCB		12.97		14.96	17.63
10OCB		14.13	14.56		18.54

Table 1(b). Time of Peak of Transitions for Cooling with 5 °C/min Ramp Rate

Sample	t_pre (min)	t_k (min)	t_post (min)	t_Sm (min)	t_N (min)
6OCB		35.21			26.58
8OCB		36.65	36.33	28.21	25.62
10OCB		34.34			24.96

Seen above in Tables 1a and 1b are the time of peak transitions for both heating and cooling of 6OCB, 8OCB, and 10OCB. The ramp rate of both heating and cooling in DSC was set to 5 °C/min. Peaks were examined in the Logger Pro application and can be seen in the graphs above. After examining the HF vs temperature and HF vs time, graphs were made to examine the HF vs Cp for all three samples as well, and can be seen below.

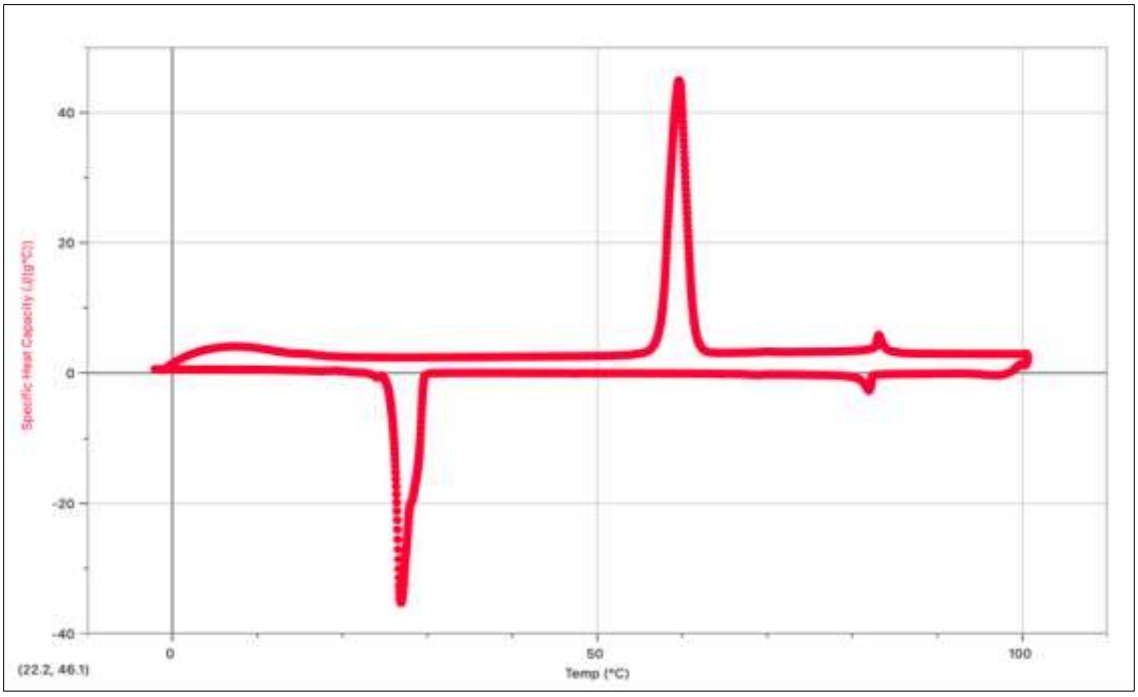

Fig. 18 Specific Heat Capacity (Cp) vs Temperature (T) graph of 8OCB sample, heating and cooling.

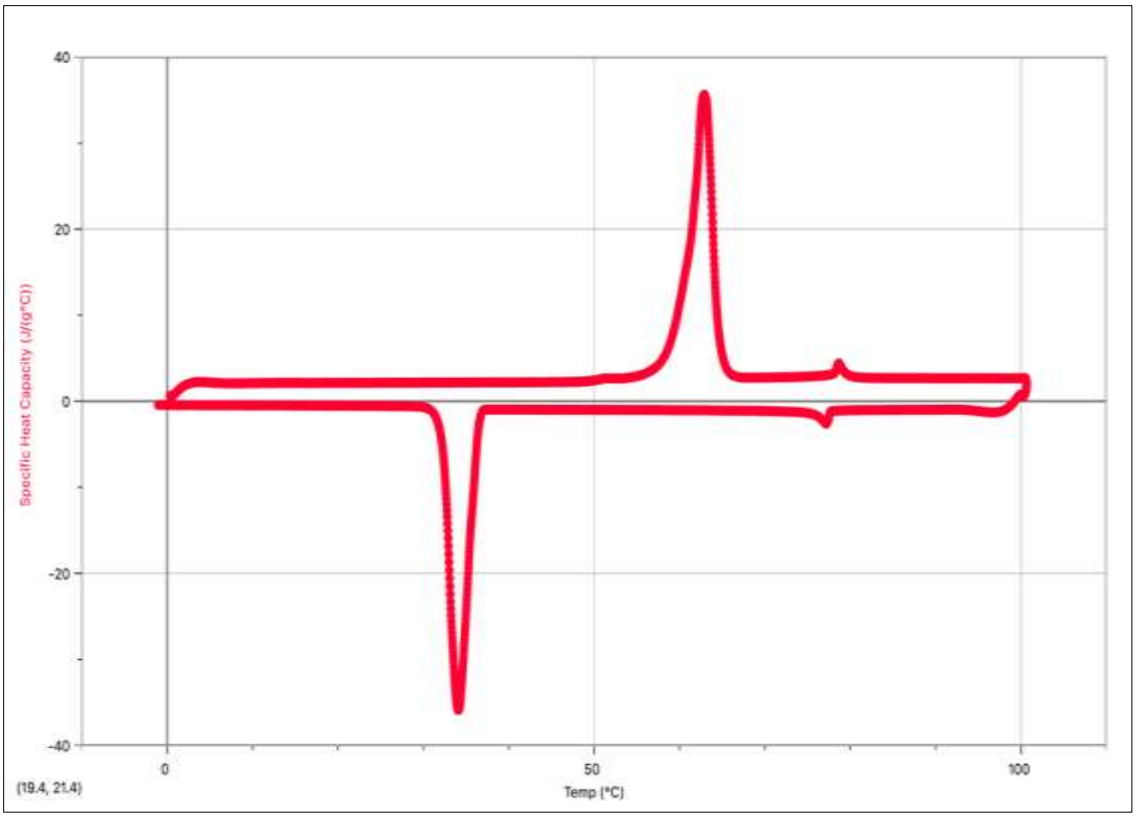

Fig. 19 Specific Heat Capacity (Cp) vs Temperature (T) graph of 6OCB sample, heating and cooling.

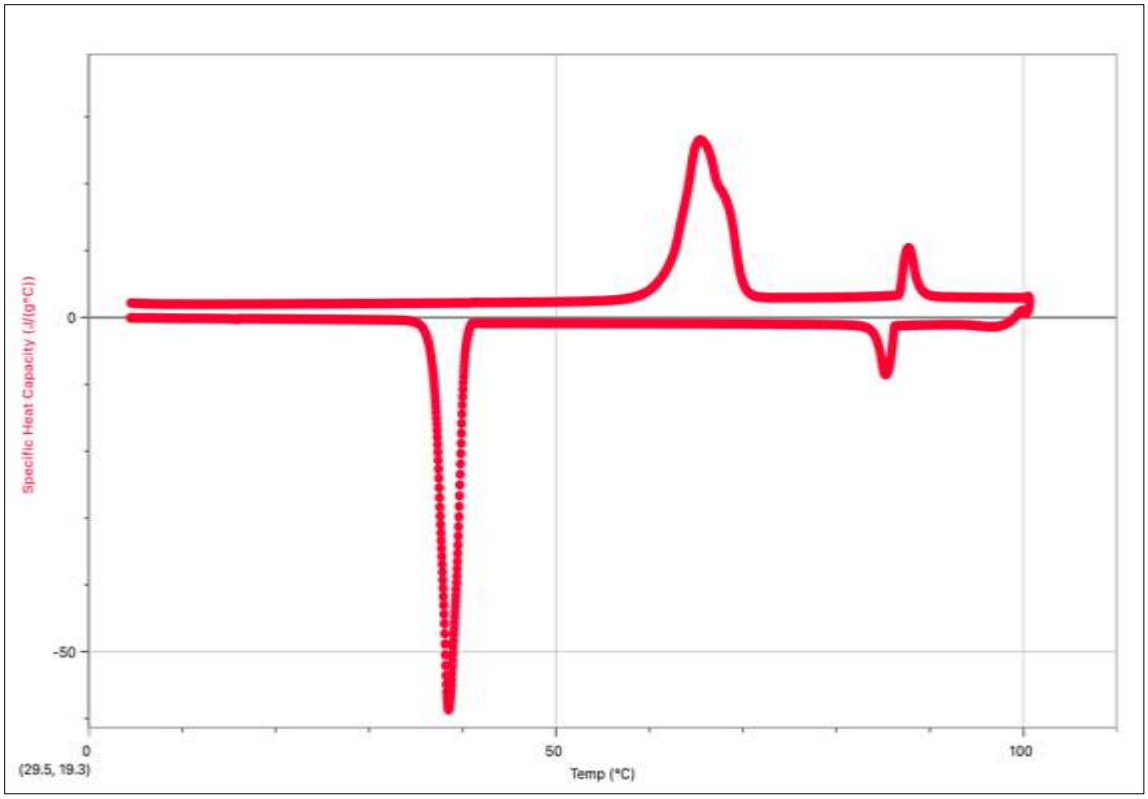

Fig. 20 Specific Heat Capacity (Cp) vs Temperature (T) graph of 10OCB sample, heating and cooling.

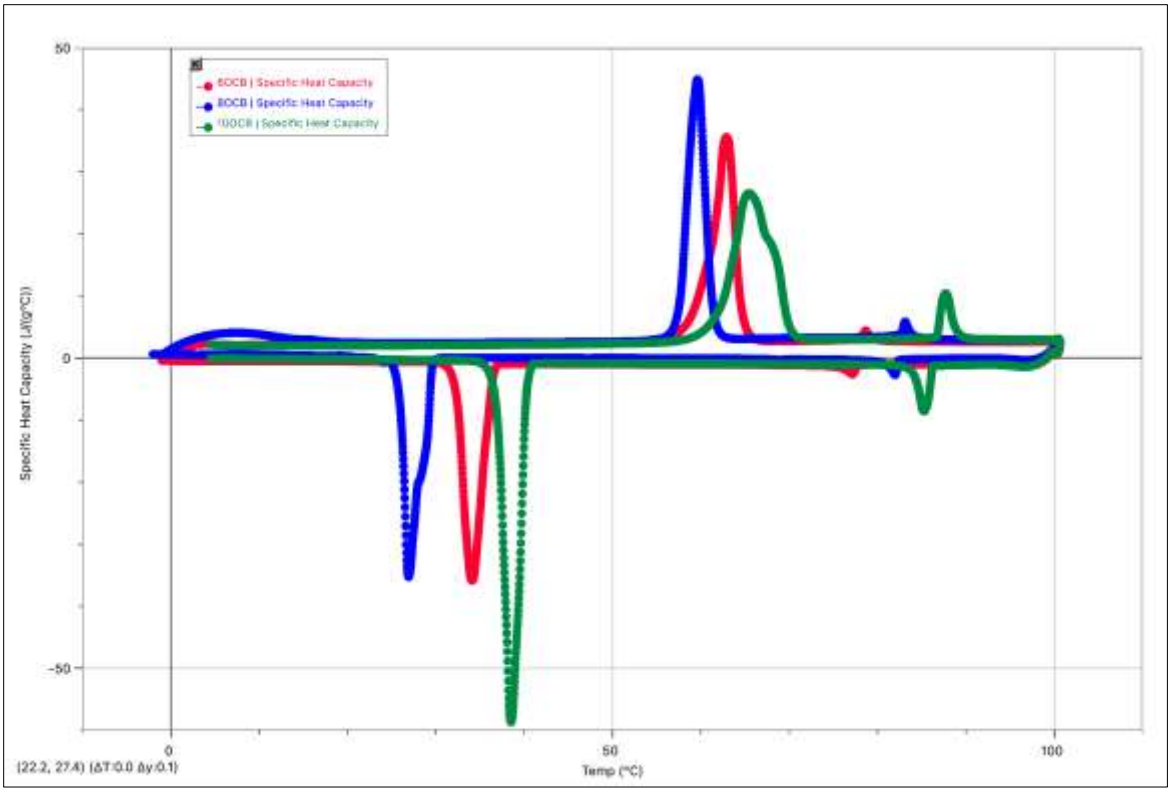

Fig. 21 Specific Heat Capacity (Cp) vs Temperature (T) graph of all three samples, 6OCB, 8OCB, and 10OCB for heating and cooling.

The amount of heat energy required to raise the temperature of 1 gram of a substance by 1°C is known as Specific Heat Capacity (Cp) [13]. The Cp was found by multiplying the heat flow (HF) by 12, specifically for the adjustment of heat flow to correspond to the rate of 1 °C/s, from 5°C/min. The Cp of 8OCB, 6OCB, and 10OCB can be seen in Figures 18, 19, and 20, respectively. These figures are seen to showcase the same patterns of phase change transitions, as seen in Figures 10, 11, and 12, displaying the HF vs temperature of each sample.

Figure 21 can be seen to examine all 3 nOCB samples' specific heat capacity together. In heating, it can again be observed that each sample exhibits the crystalline phase first, with 8OCB appearing to display the crystalline peak first, followed by 6OCB, and lastly 10OCB. The crystalline peaks display the same patterns observed in the HF vs temperature figures, with 6OCB having a small and wide crystalline peak, 10OCB having a much shorter and wider crystalline peak, and 8OCB having the sharpest and tallest crystalline peak. Once again, only 8OCB is shown to exhibit a Smectic A peak, following the crystalline peak. The nematic peaks can be seen next with 6OCB first, then 8OCB, and finally 10OCB. The 6OCB can be seen to have the smallest nematic peak, and 10OCB shows the largest and widest nematic peak, compared to 8OCB, which can be seen to have an intermediate-sized nematic peak. While heating the samples, we can again observe a short temperature range between the crystalline peaks and nematic peaks. The isotropic phase for all nOCB samples can be seen after the nematic peaks. In cooling, it can once again be observed that each sample displays a nematic phase first, following the isotropic phase.

The 10OCB LC shows this nematic peak first, being the largest and widest, and 6OCB can be seen showing the smallest and narrowest nematic peak last, compared to 8OCB, showing an intermediate-sized nematic peak between 6OCB and 10OCB. Again, the smectic A phase is only observed in the 8OCB sample, after the nematic peaks. In cooling as well, all three nOCB liquid crystals exhibit a crystalline phase. The 10OCB sample can be seen first, showing a very large and sharp peak, then 6OCB can be seen next, showing a shorter and wider peak, and 8OCB is lastly seen, showing the shortest and widest double peak. While cooling the samples, we again observe a much larger temperature range between the crystalline and nematic peaks.

Table 2(a). Peak Values of the Cp for each transition of all three samples for Heating.

Sample	Tpre (J/g)	Tk (J/g)	Tpost (J/g)	TSm (J/g)	TN (J/g)
6OCB	3.1	35.8			4.6
8OCB		45.1		3.38	6.2
10OCB		27.2	18.7		10.9

Table 2(b). Peak Values of the Cp for each transition of all three samples for Cooling.

Sample	Tpre (J/g)	Tk (J/g)	Tpost (J/g)	TSm (J/g)	TN (J/g)
6OCB		36.2			2.8
8OCB		35.4		1.3	3.1
10OCB		59.2			

Seen above in Tables 2a and 2b are the Cp values of peak transitions for both heating and cooling of 6OCB, 8OCB, and 10OCB. The ramp rate of both heating and cooling in DSC was set to 5 °C/min. Peaks were examined in the Logger Pro application and can be seen in the graphs above as well.

Each sample was also examined more closely, looking at only heating for the HF vs temperature, and only cooling for the HF vs temperature. These graphs can be seen below in Figures 22-26.

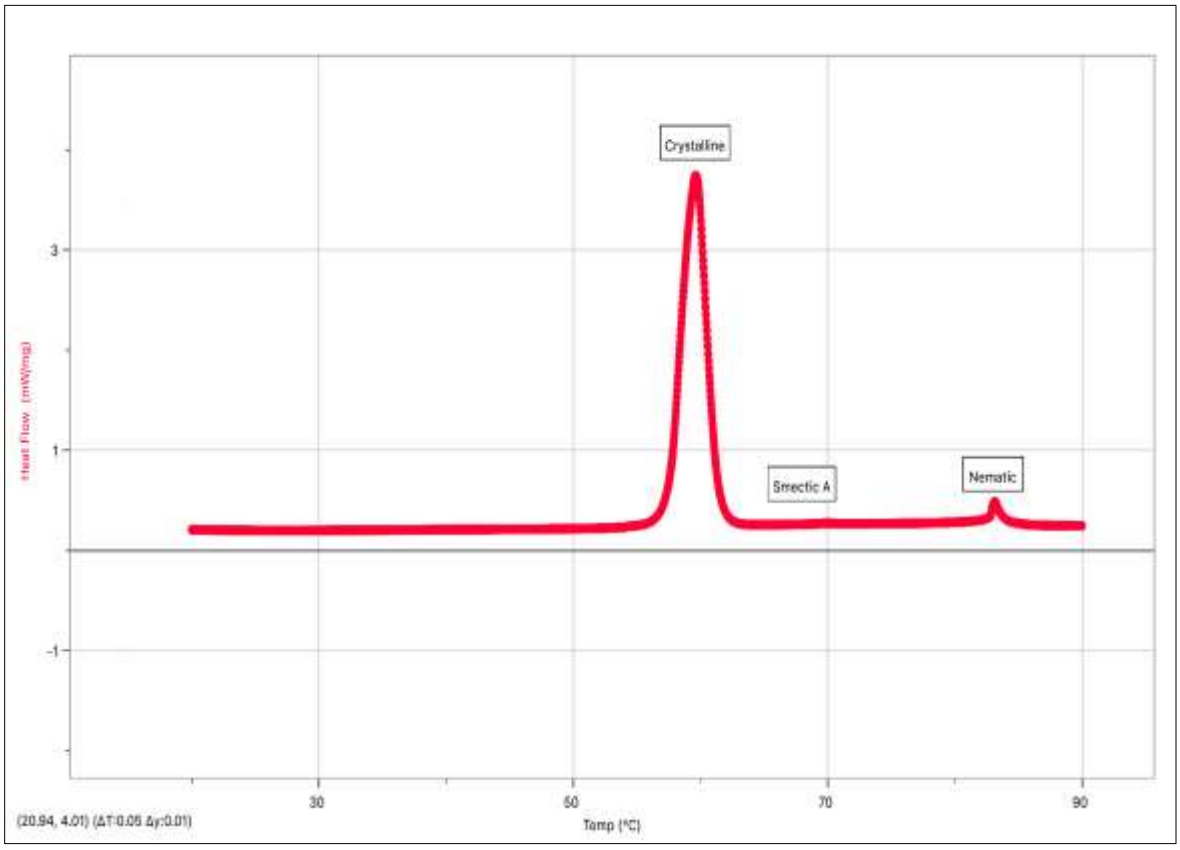

Fig. 22 Heat Flow (HF) vs Temperature (T) graph of 8OCB sample, heating only.

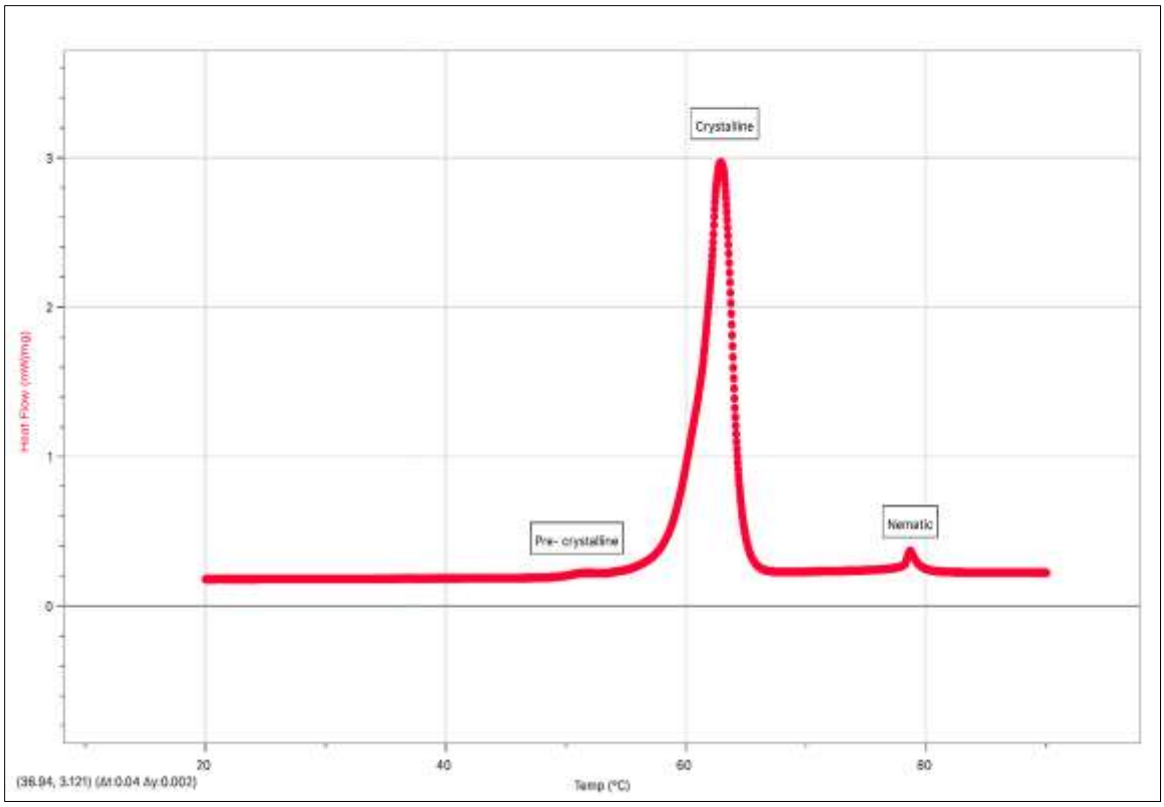

Fig. 23 Heat Flow (HF) vs Temperature (T) graph of 6OCB sample, heating only.

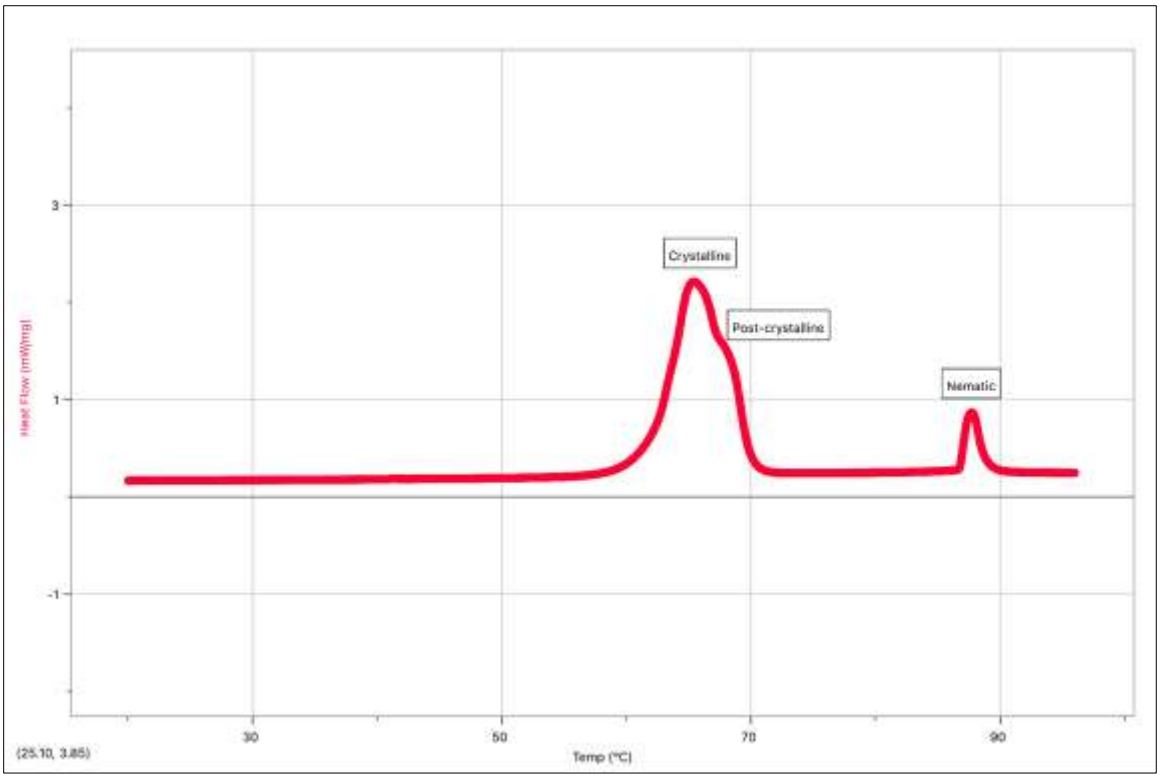

Fig. 24 Heat Flow (HF) vs Temperature (T) graph of 10OCB sample, heating only.

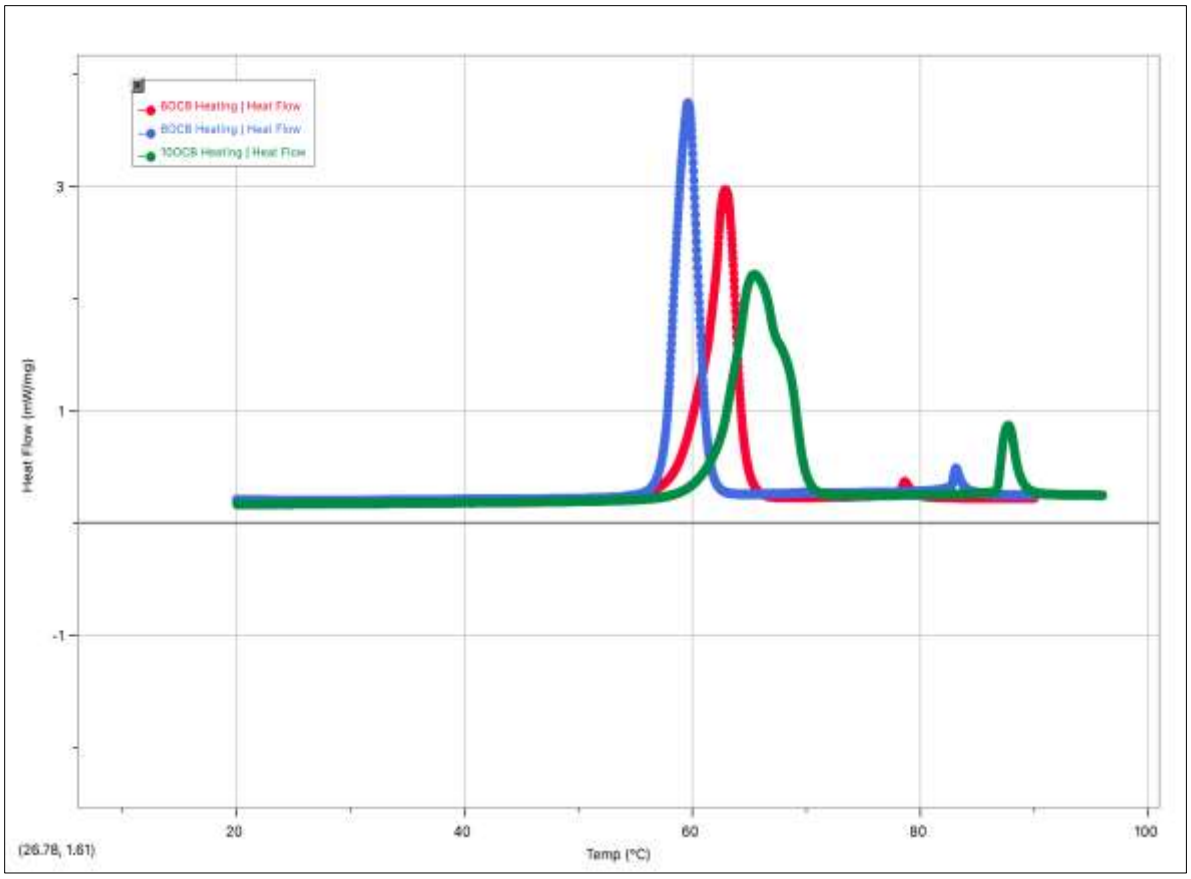

Fig. 25 Heat Flow (HF) vs Temperature (T) graph of all three samples, 6OCB, 8OCB, and 10OCB, heating only.

In more closely examining the phase change transitions of 8OCB, 6OCB, and 10OCB, in Figures 22-25, we can see each LC behaving differently and in an interesting manner during heating. As established previously, in heating, each sample can be seen to display a crystalline, nematic, and isotropic phase, with 8OCB being the only sample to show a smectic A phase. As seen above in Figure 23, the 6OCB sample exhibits a pre-crystalline peak, while in Figure 24, the 10OCB sample exhibits a post-crystalline peak, instead of a smectic A peak, as seen in 8OCB. The appearance of the smectic A phase in 8OCB, compared to no evidence of a smectic A phase in 6OCB and 10OCB, can be seen below in Figure 38. Figure 30 shows a zoomed-in image of the pre-crystalline peak discovered in the 6OCB HF vs temperature graph. Figure 34 shows a zoomed-in image of the post-crystalline peak discovered in the 10OCB HF vs temperature graph.

Table 3. Peak Temperature of all Transitions of all samples for Heating with 5 °C/min Ramp Rate.

Sample	Tpre (°C)	Tk (°C)	Tpost (°C)	TSm (°C)	TN (°C)
6OCB	51.36	62.9			78.74
8OCB		59.63		69.81	83.14
10OCB		65.49	68.55		87.76

Seen above in Table 3 are the temperatures of peak transitions for heating of 6OCB, 8OCB, and 10OCB, with the ramp rate in DSC being set to 5 °C/min. Peaks were examined in the Logger Pro application and can be seen in the graphs above.

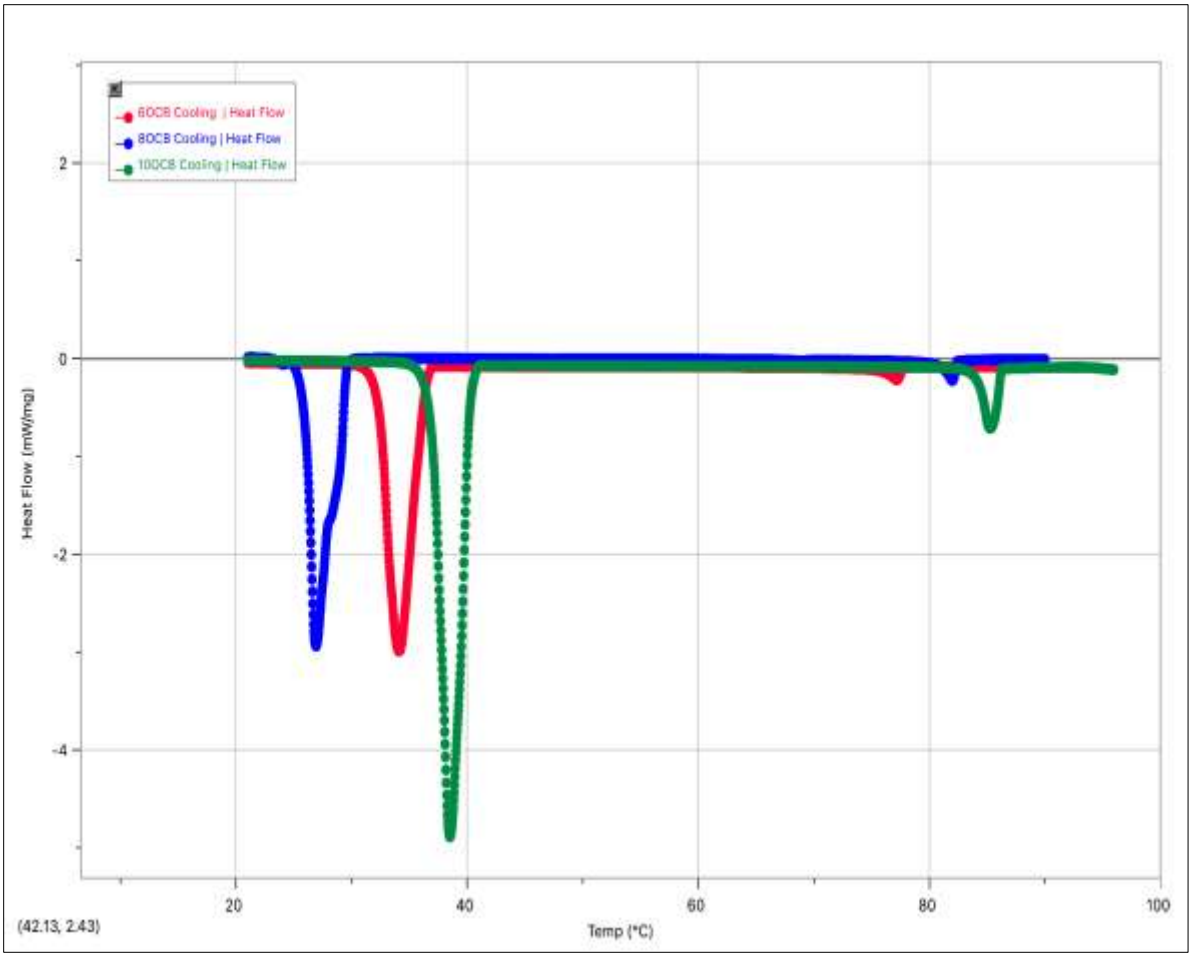

Fig. 26 Heat Flow (HF) vs Temperature (T) graph of all three samples, 6OCB, 8OCB, and 10OCB, cooling only.

In more closely examining the phase change transitions of 8OCB, 6OCB, and 10OCB, in Figure 26, we can again see each LC behaving interestingly during cooling. As previously mentioned, in cooling, each sample can be seen to display a crystalline, nematic, and isotropic phase, with 8OCB being the only sample to show a smectic A phase. Evidence showing no appearance of a smectic A phase in 6OCB and 10OCB in cooling, compared to 8OCB, can be seen below in Figure 50. In cooling, however, 6OCB does not retain a pre-crystalline peak, as seen more closely in Figure 42, and 10OCB does not retain a post-crystalline peak as seen in Figure 46.

Table 4. Peak Temperature of all Transitions for all samples for Cooling with 5 °C/min Ramp Rate.

Sample	Tpre (°C)	Tk (°C)	Tpost (°C)	TSm (°C)	TN (°C)
6OCB		34.17			77.19
8OCB	28.31	26.93		69.01	82.02
10OCB		38.52			85.29

Seen above in Table 4 are the temperatures of peak transitions for the cooling of 6OCB, 8OCB, and 10OCB, with the ramp rate in DSC being set to 5 °C/min. Peaks were examined in the Logger Pro application and can be seen in the graphs above.

Each phase change transition was also examined more closely by zooming in on each peak for the three samples in both heating and cooling.

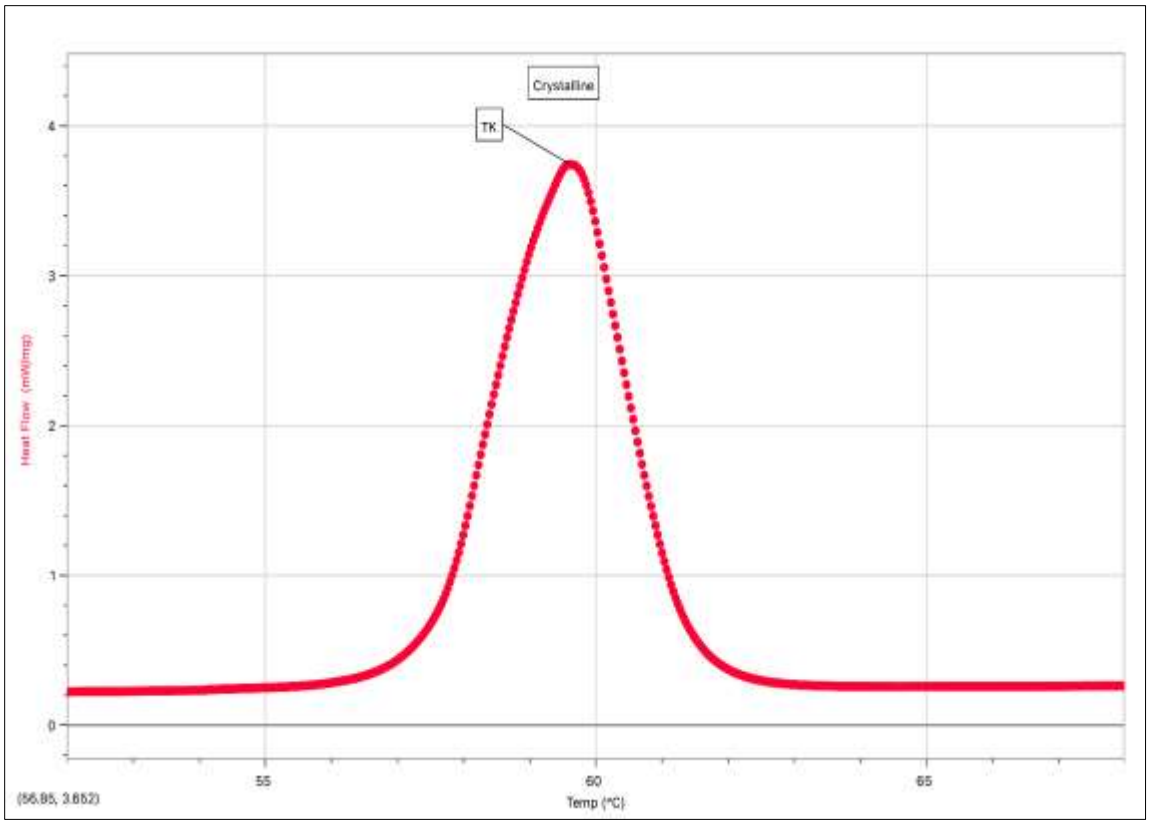

Fig. 27 Zoomed-in graph of Heat Flow (HF) vs Temperature (T) crystalline phase in 8OCB sample, in heating.

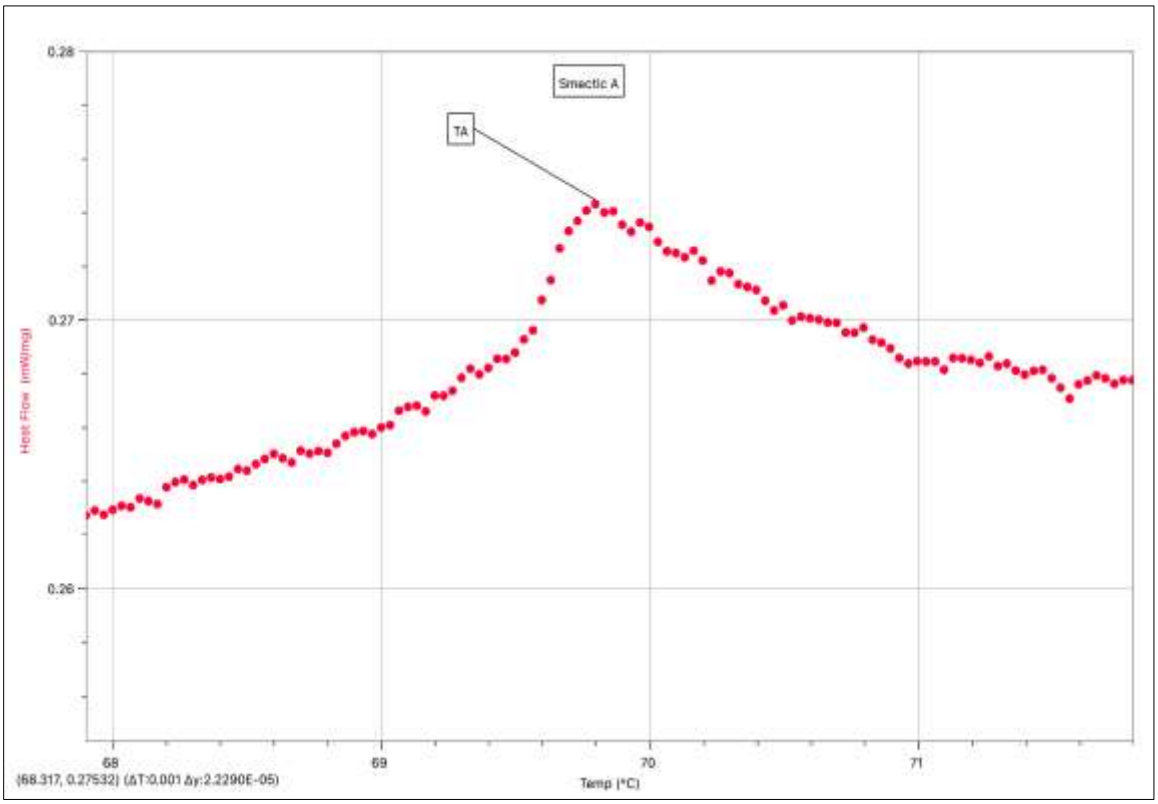

Fig. 28 Zoomed-in graph of Heat Flow (HF) vs Temperature (T) Smectic A phase in 8OCB sample, in heating.

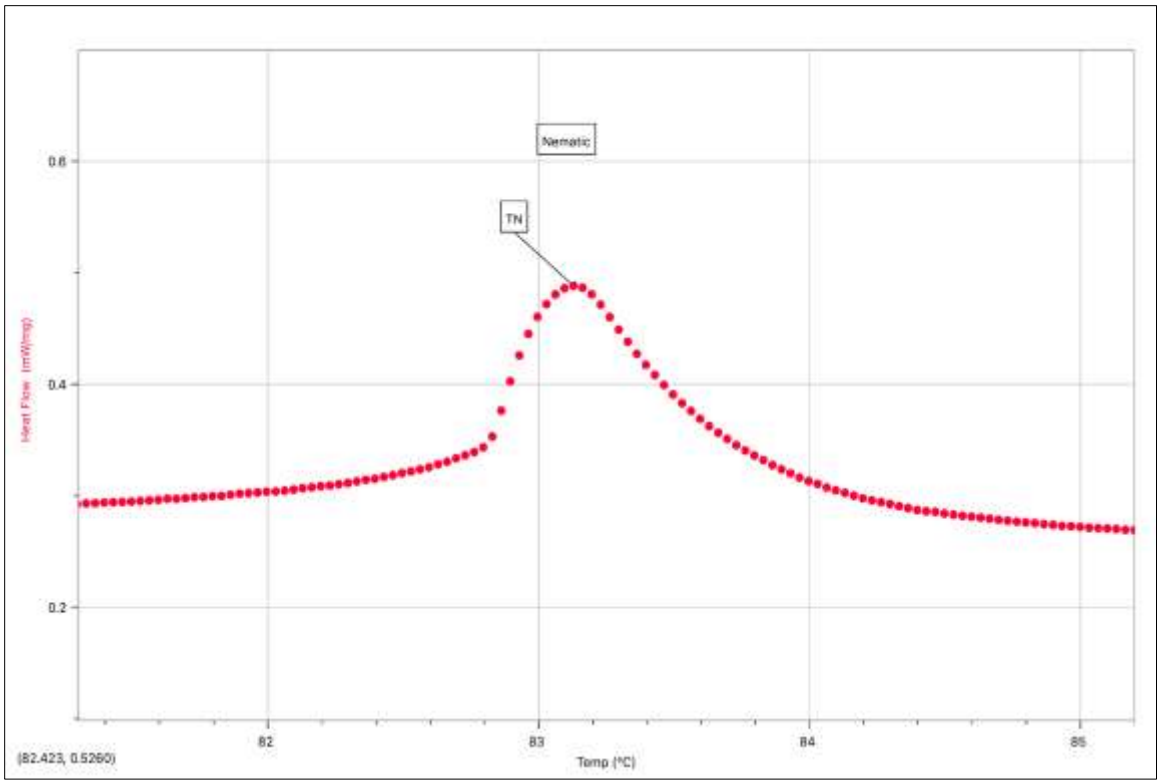

Fig. 29 Zoomed-in graph of Heat Flow (HF) vs Temperature (T) nematic phase in 8OCB sample, in heating.

In Figures 27-29, zoomed-in images of all important peaks of phase change transitions of 8OCB found when analyzing the sample during heating can be seen. Figure 27 highlights the crystalline phase, Figure 28 highlights the smectic A phase, and Figure 29 highlights the nematic phase.

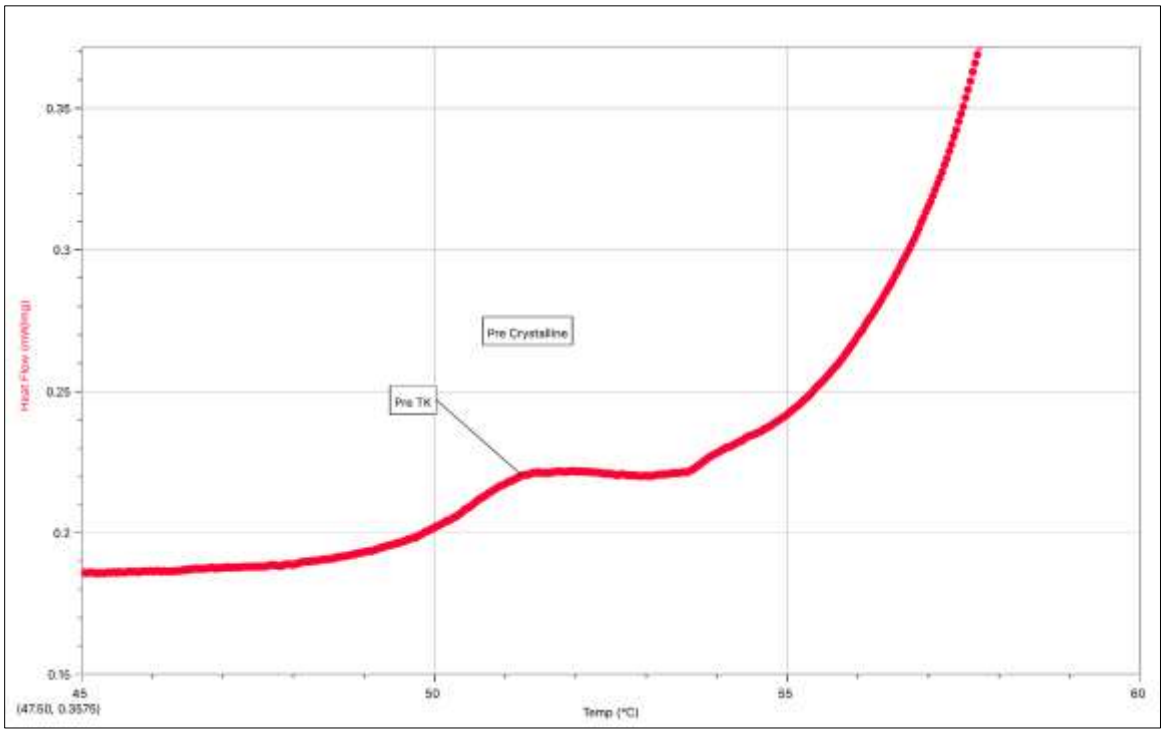

Fig. 30 Zoomed-in graph of Heat Flow (HF) vs Temperature (T) of pre-crystalline phase in 6OCB sample, in heating.

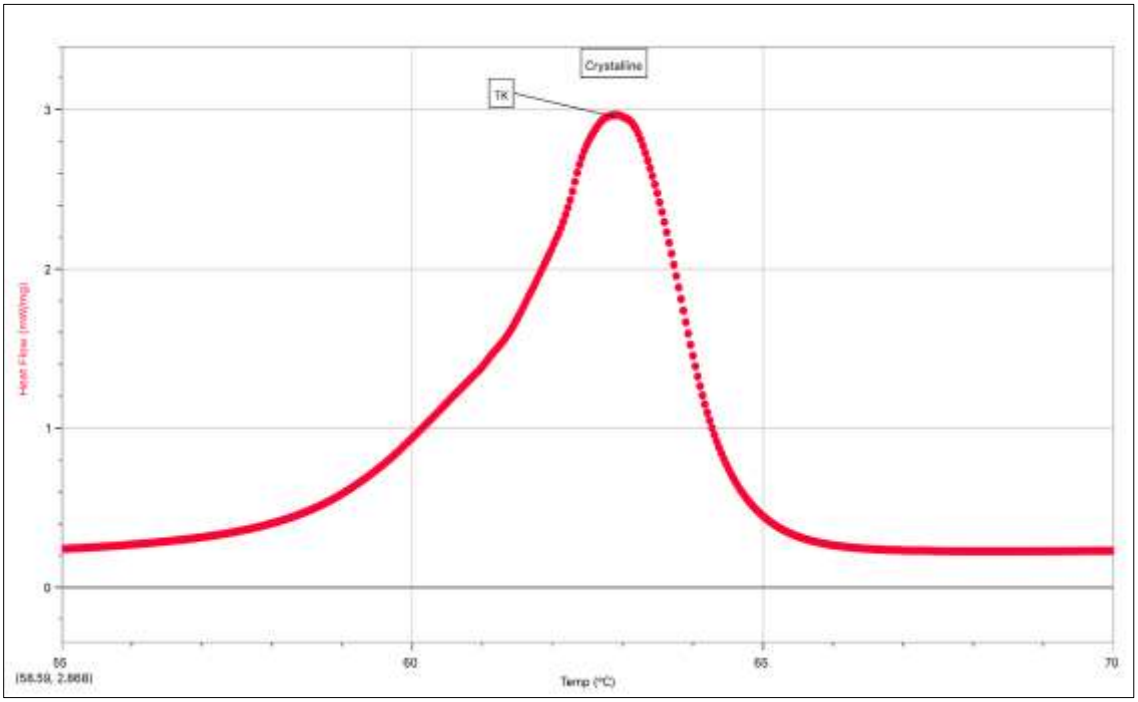

Fig. 31 Zoomed-in graph of Heat Flow (HF) vs Temperature (T) crystalline phase in 6OCB sample, in heating.

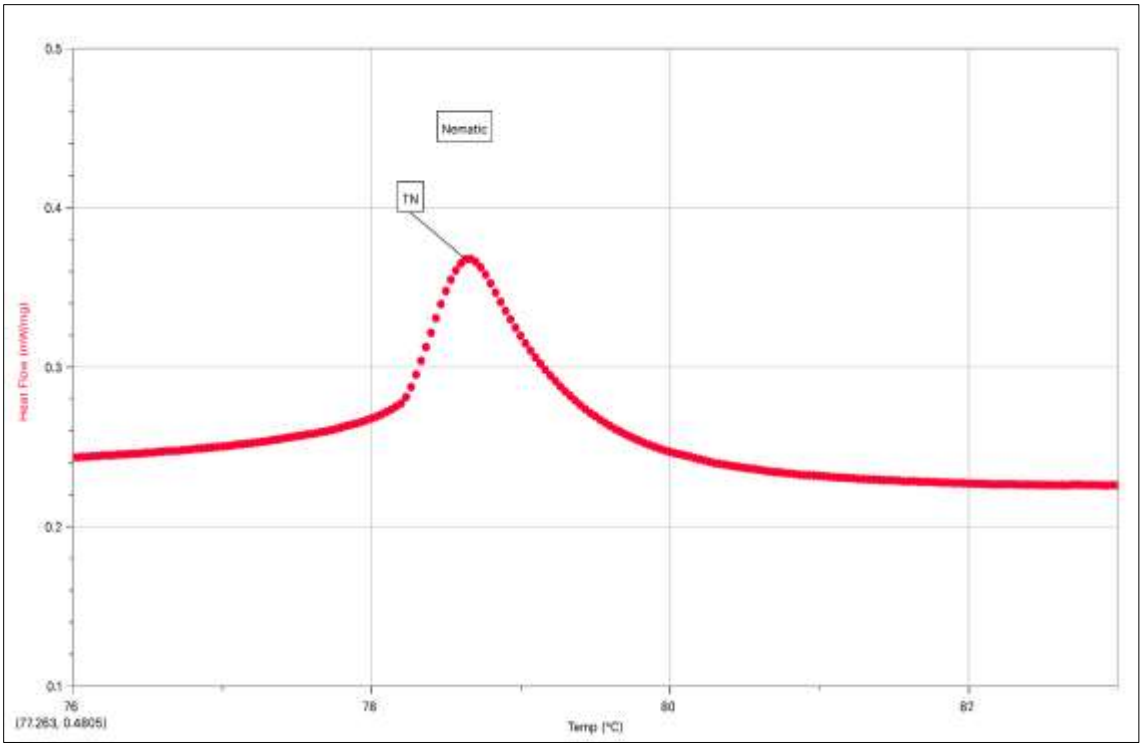

Fig. 32 Zoomed-in graph of Heat Flow (HF) vs Temperature (T) nematic phase in 6OCB sample, in heating.

In Figures 30-32, zoomed-in images of all important peaks of phase change transitions of 6OCB found when analyzing the sample during heating can be seen. Figure 30 highlights the pre-crystalline phase, Figure 31 highlights the crystalline phase, and Figure 32 highlights the nematic phase.

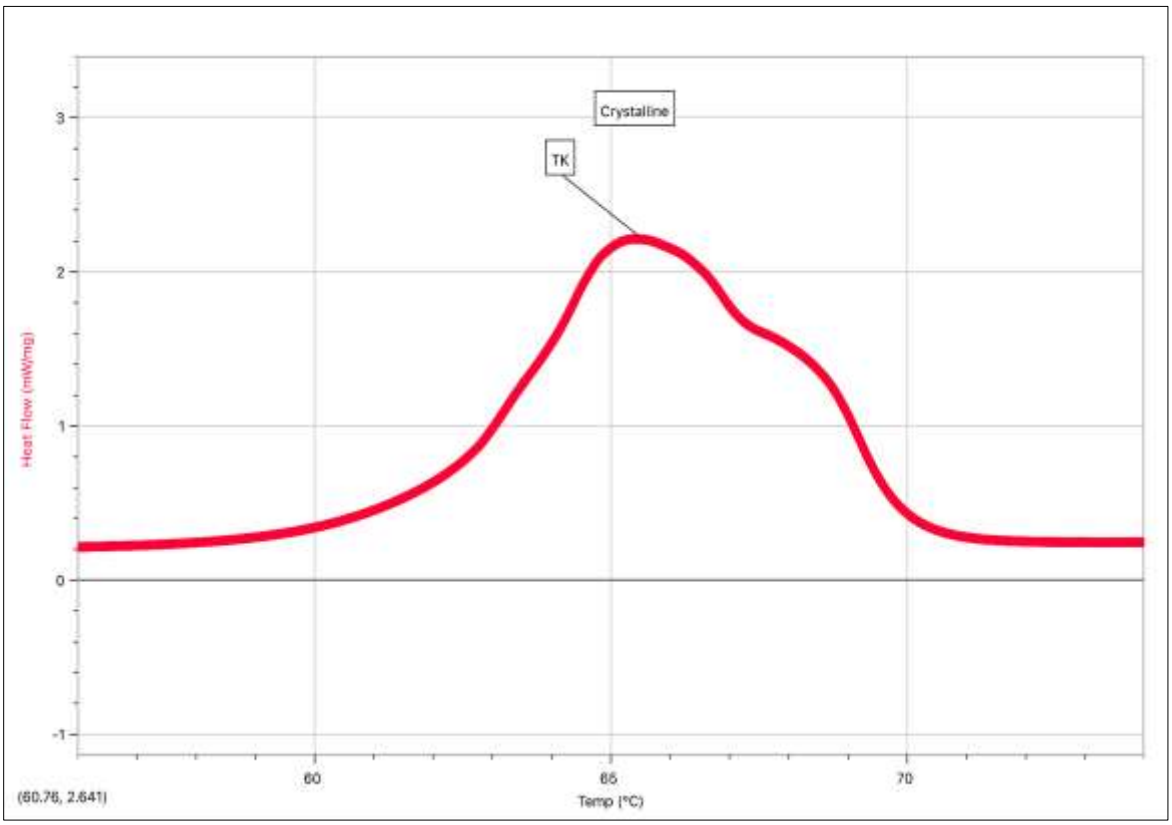

Fig. 33 Zoomed-in graph of Heat Flow (HF) vs Temperature (T) crystalline phase in 10OCB sample, in heating.

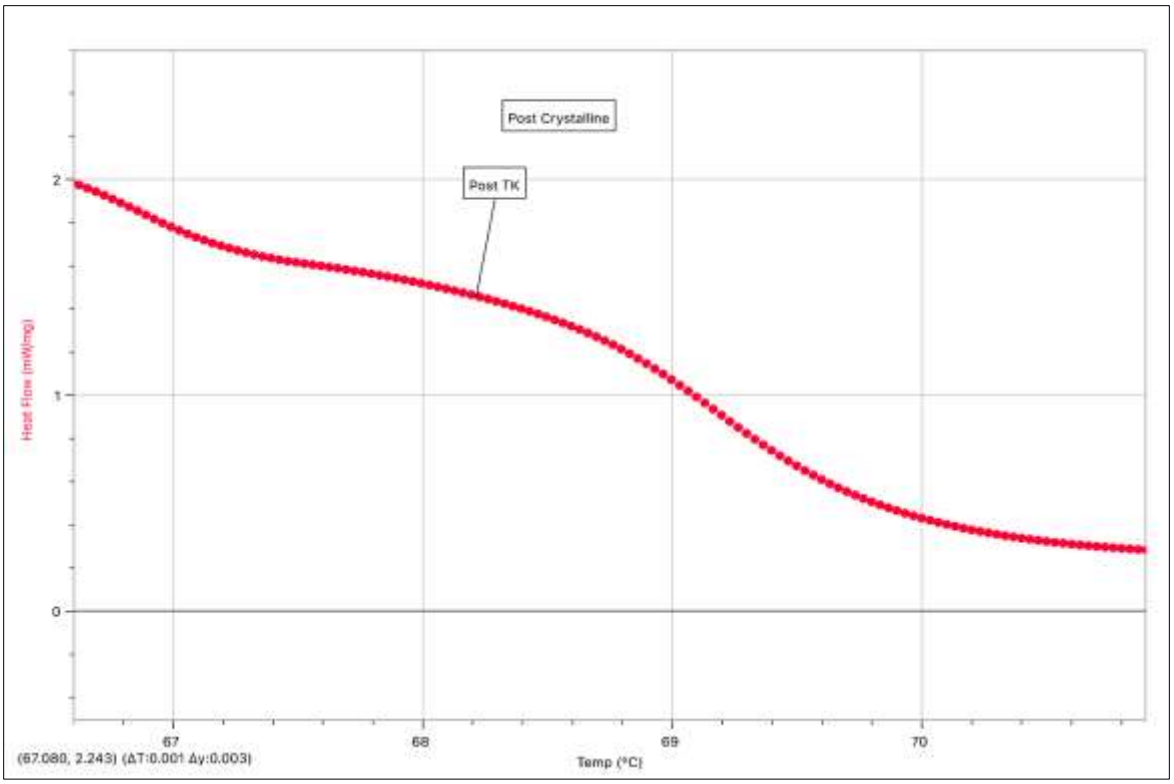

Fig. 34 Zoomed-in graph of Heat Flow (HF) vs Temperature (T) post-crystalline phase in 10OCB sample, in heating.

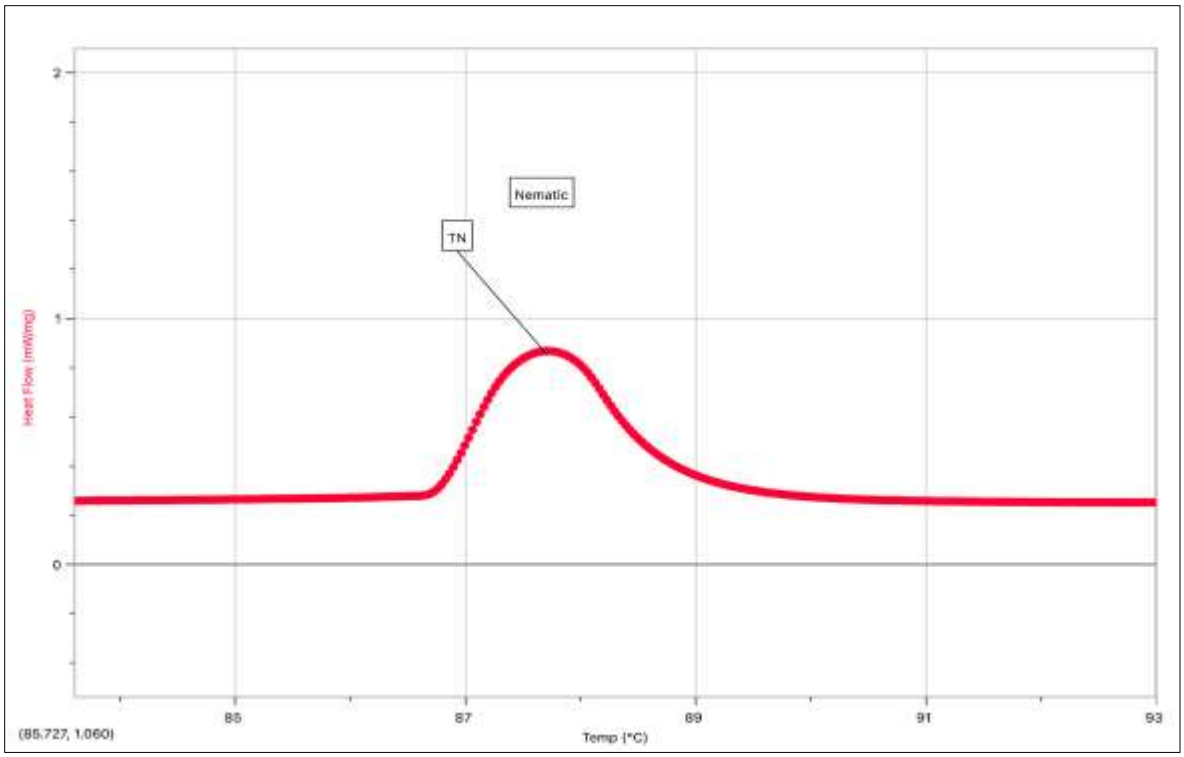

Fig. 35 Zoomed-in graph of Heat Flow (HF) vs Temperature (T) nematic phase in 10OCB sample, in heating.

In Figures 33-35, zoomed-in images of all important peaks of phase change transitions of 10OCB found when analyzing the sample in heating can be seen. Figure 33 highlights the crystalline phase, Figure 34 highlights the post-crystalline phase, and Figure 35 highlights the nematic phase.

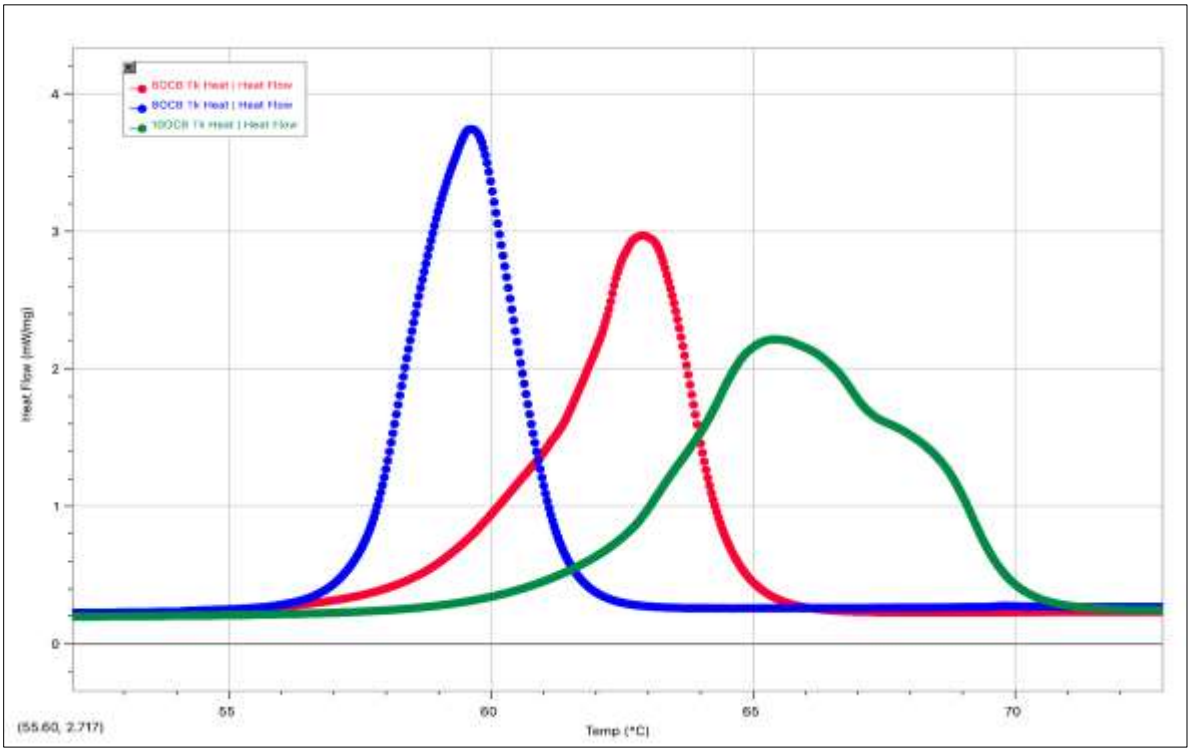

Fig. 36 Zoomed-in graph of Heat Flow (HF) vs Temperature (T) for crystalline phase for all three samples, 6OCB, 8OCB, and 10OCB, heating only.

Seen above in Figure 36 is a comparison of the crystalline phase of all three samples during heating. It can clearly be seen that 8OCB experiences the crystalline phase first, with a large, sharp peak, followed by 6OCB, with a shorter yet still large peak, and finally 10OCB, with a very short and wide peak.

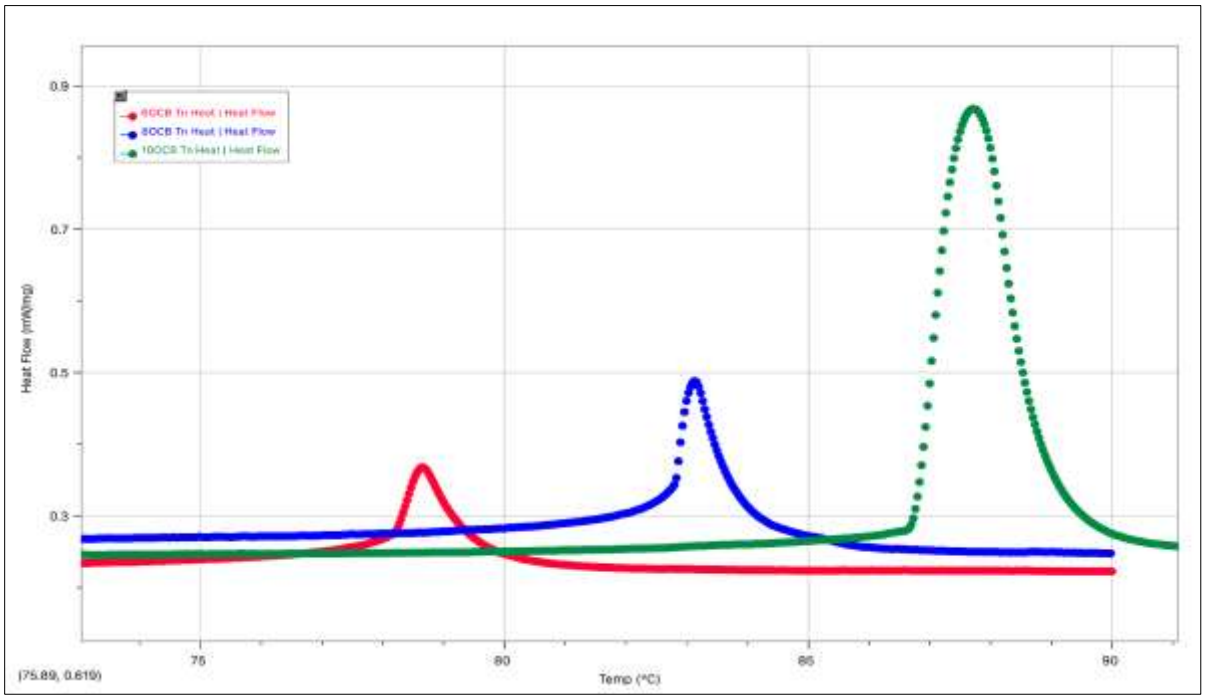

Fig. 37 Zoomed-in graph of Heat Flow (HF) vs Temperature (T) for the nematic phase for all three samples, 6OCB, 8OCB, and 10OCB, heating only.

Comparison of nematic peaks for all three samples can be seen above in **Figure 37** during heating. It can be observed that 6OCB displays a short nematic peak first, followed by 8OCB with a taller nematic peak, and finally 10OCB with a much larger, taller, and wider nematic peak.

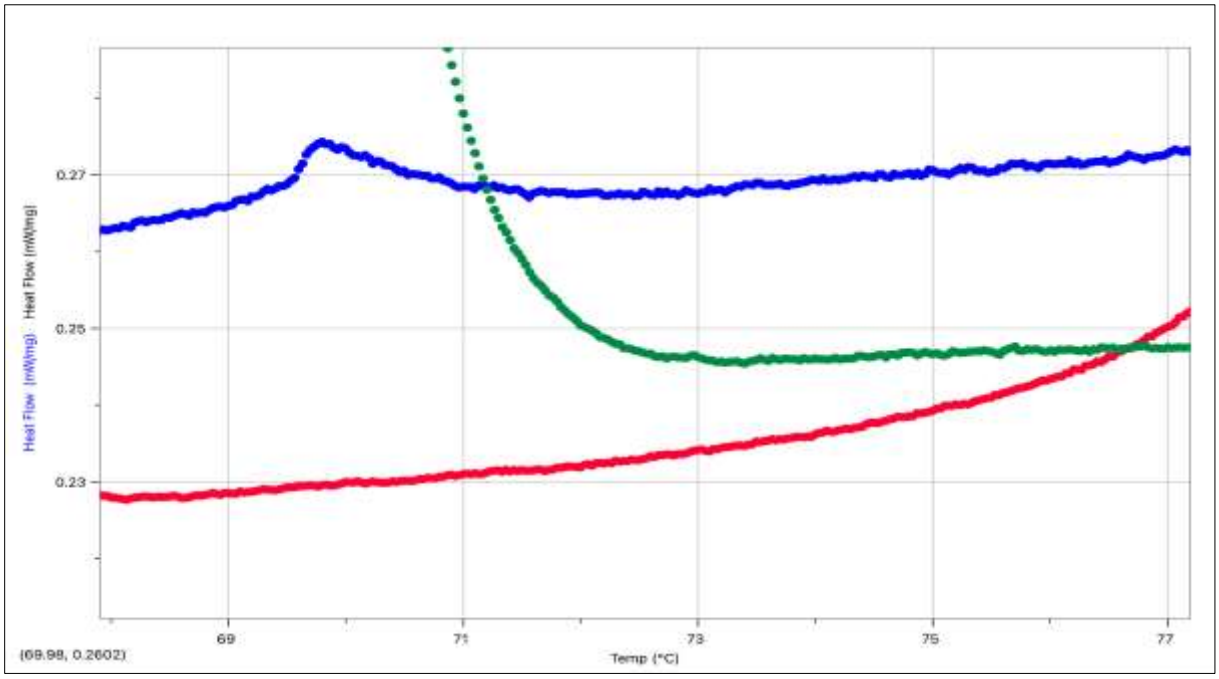

Fig. 38 Comparison of Smectic A in the 8OCB sample to no evidence of Smectic A in 6OCB and 10OCB samples, in heating.

As seen above in Figure 38, the comparison of the smectic A phase in heating, the only sample of the three to experience a smectic A phase is 8OCB. The 6OCB and 10OCB samples do not display a smectic A phase when heating.

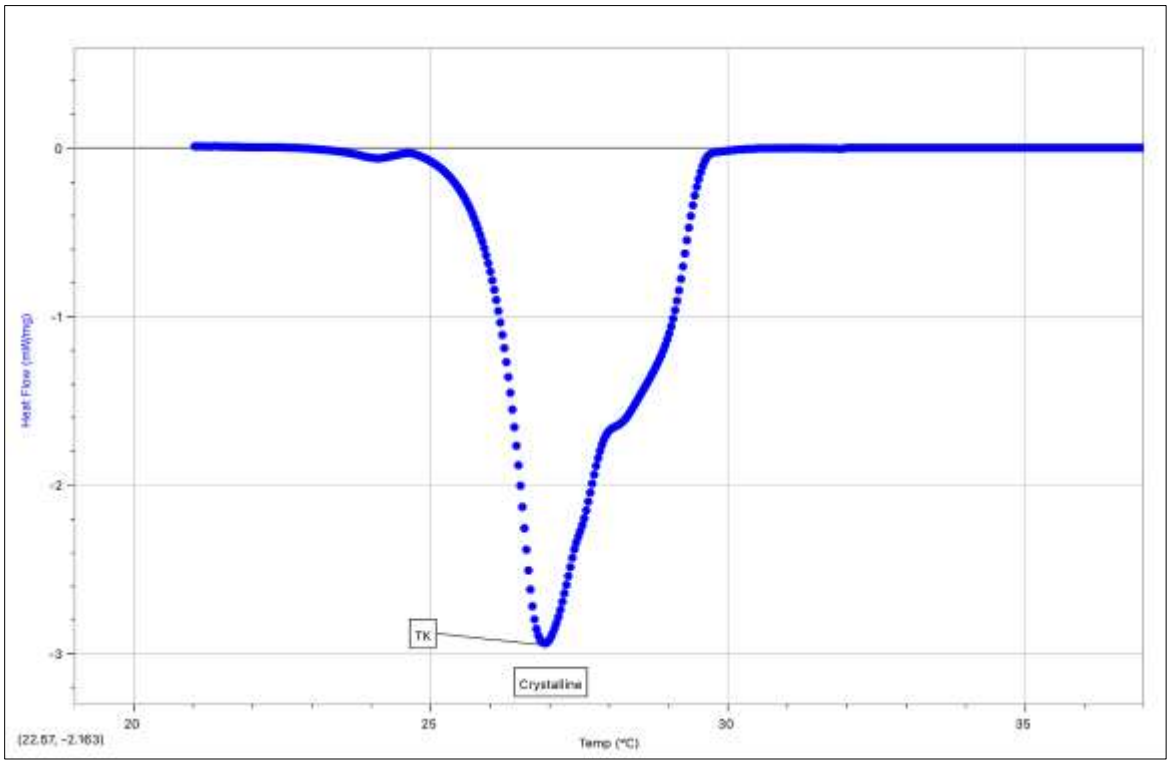

Fig. 39 Zoomed-in graph of Heat Flow (HF) vs Temperature (T) crystalline phase in 8OCB sample, in cooling.

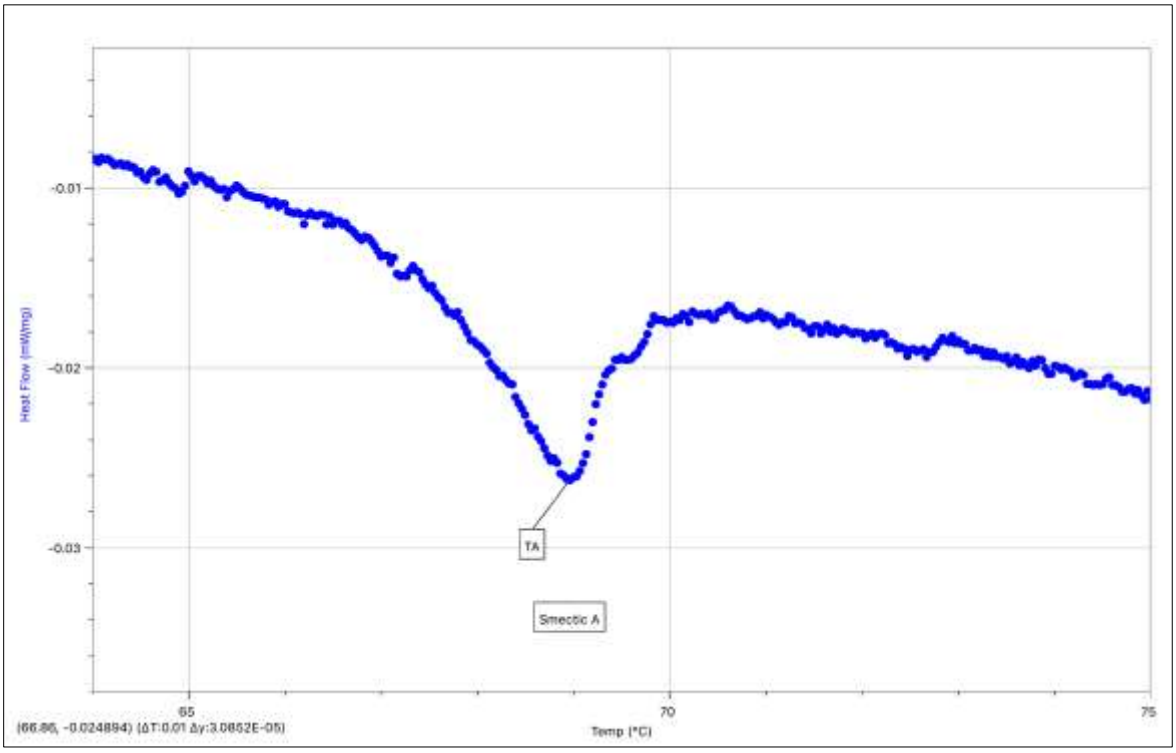

Fig. 40 Zoomed-in graph of Heat Flow (HF) vs Temperature (T) Smectic A phase in 8OCB sample, in cooling.

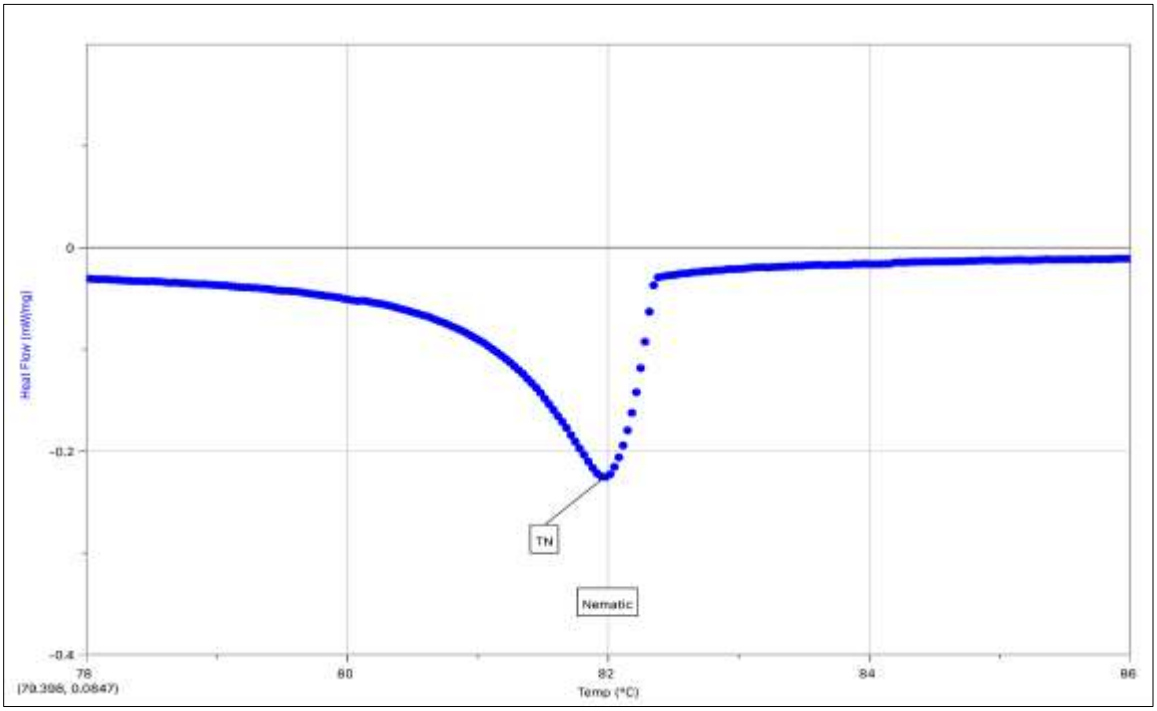

Fig. 41 Zoomed-in graph of Heat Flow (HF) vs Temperature (T) nematic phase in 8OCB sample, in cooling.

In Figures 39-41, zoomed-in images of all important peaks of phase change transitions of 8OCB found when analyzing the sample in cooling can be seen. Figure 39 highlights the crystalline phase, Figure 40 highlights the smectic A phase, and Figure 31 highlights the nematic phase. The crystalline phase during cooling appears to show behavior of a pre-crystalline phase, and more details can be observed from previous research. [8]

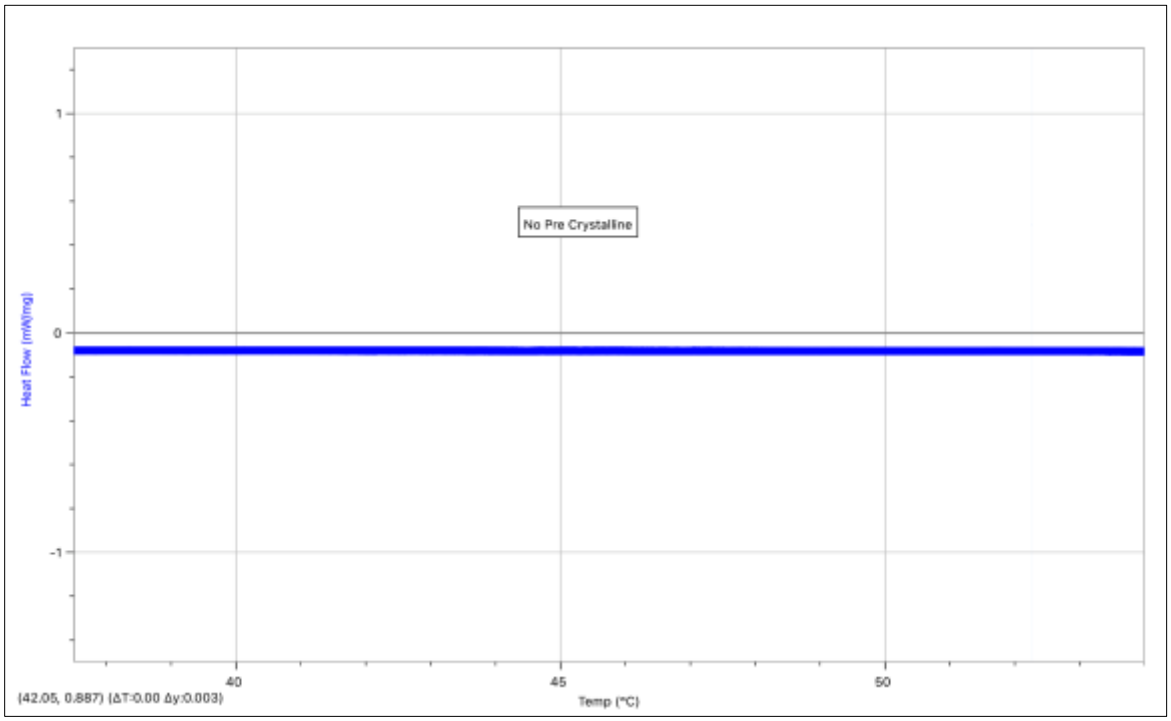

Fig. 42 Zoomed-in graph of Heat Flow (HF) vs Temperature (T) pre-crystalline phase in 6OCB sample, in cooling.

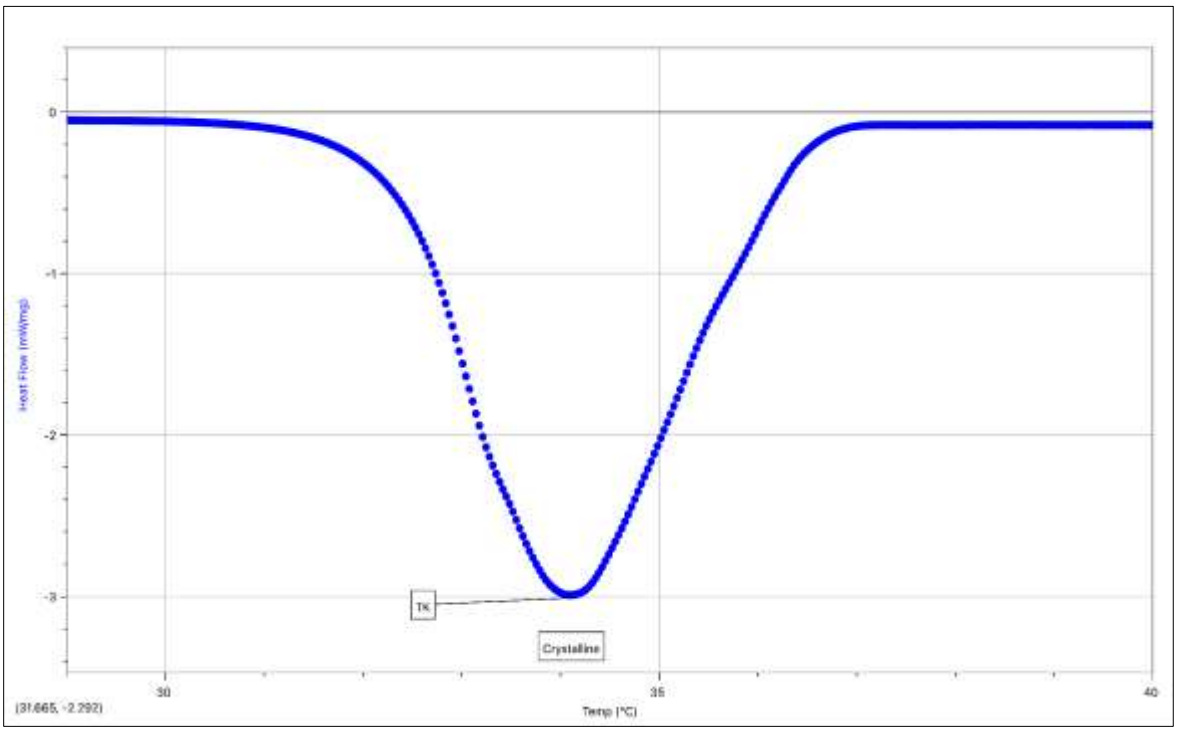

Fig. 43 Zoomed-in graph of Heat Flow (HF) vs Temperature (T) crystalline phase in 6OCB sample, in cooling.

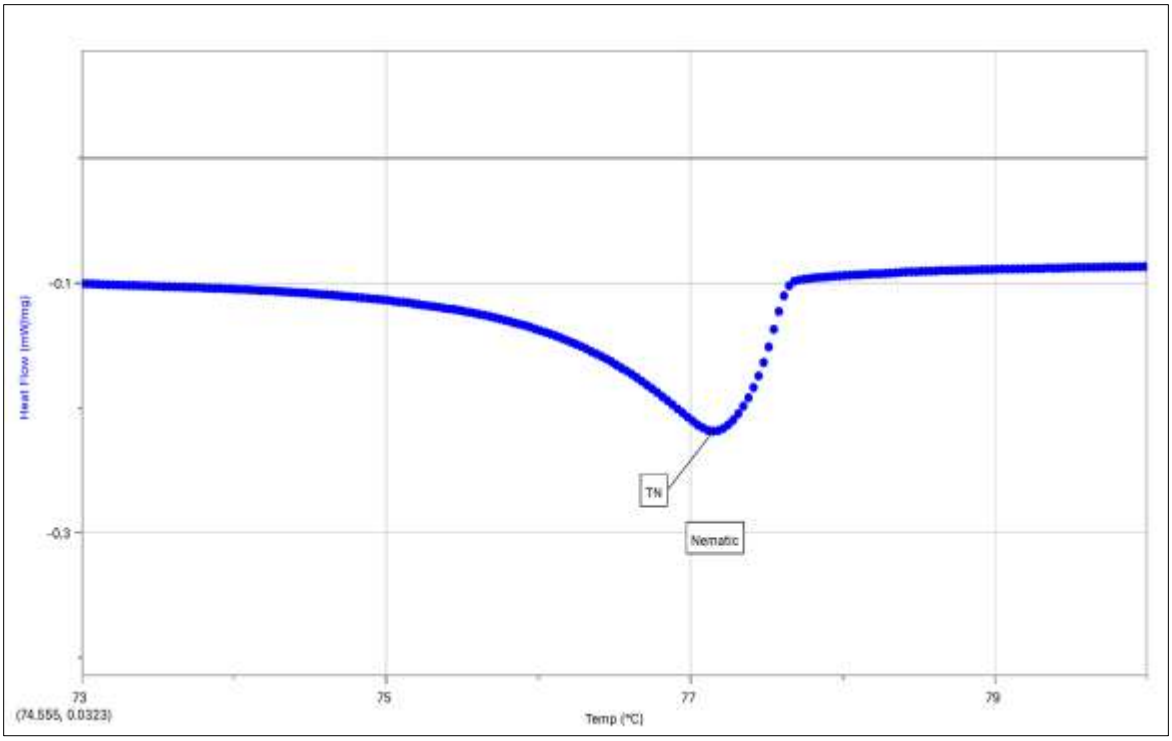

Fig. 44 Zoomed-in graph of Heat Flow (HF) vs Temperature (T) nematic phase in 6OCB sample, in cooling.

In Figures 42-44, zoomed-in images of all important peaks of phase change transitions of 6OCB found when analyzing the sample in cooling can be seen. Figure 42 highlights that there is no pre-crystalline phase, Figure 43 highlights the crystalline phase, and Figure 44 highlights the nematic phase.

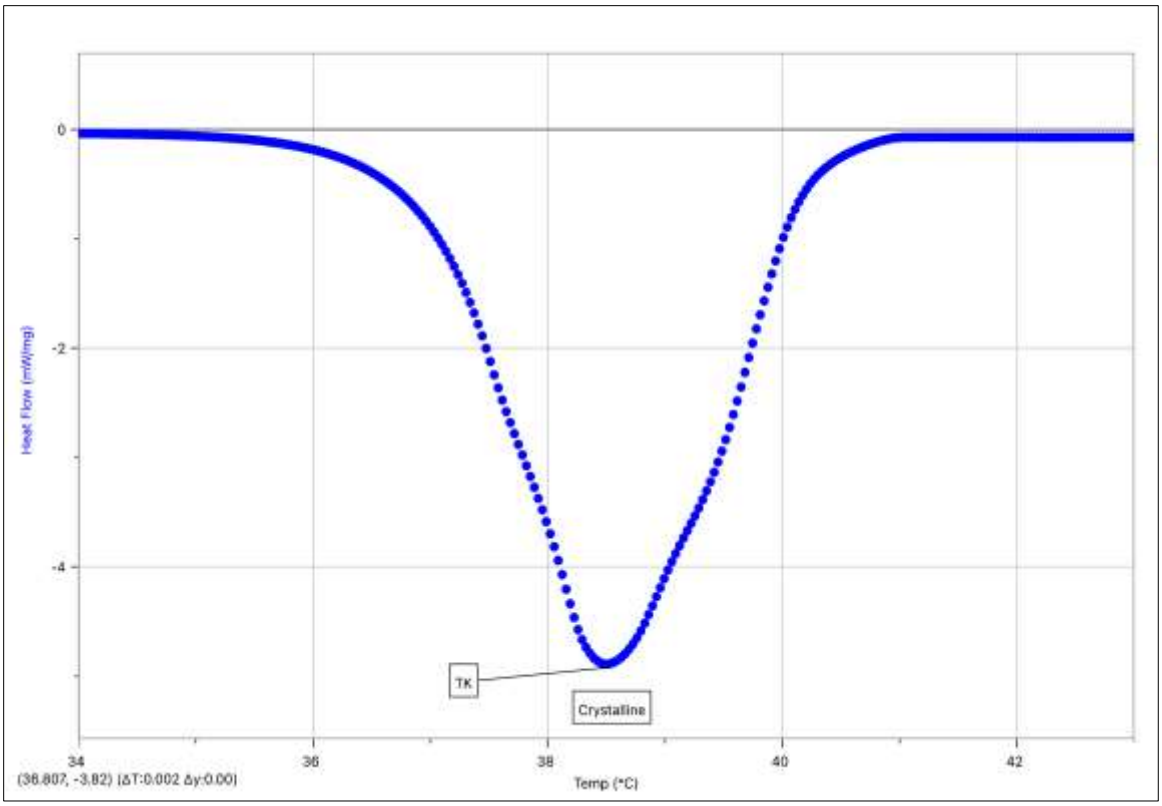

Fig. 45 Zoomed-in graph of Heat Flow (HF) vs Temperature (T) crystalline phase in 10OCB sample, in cooling.

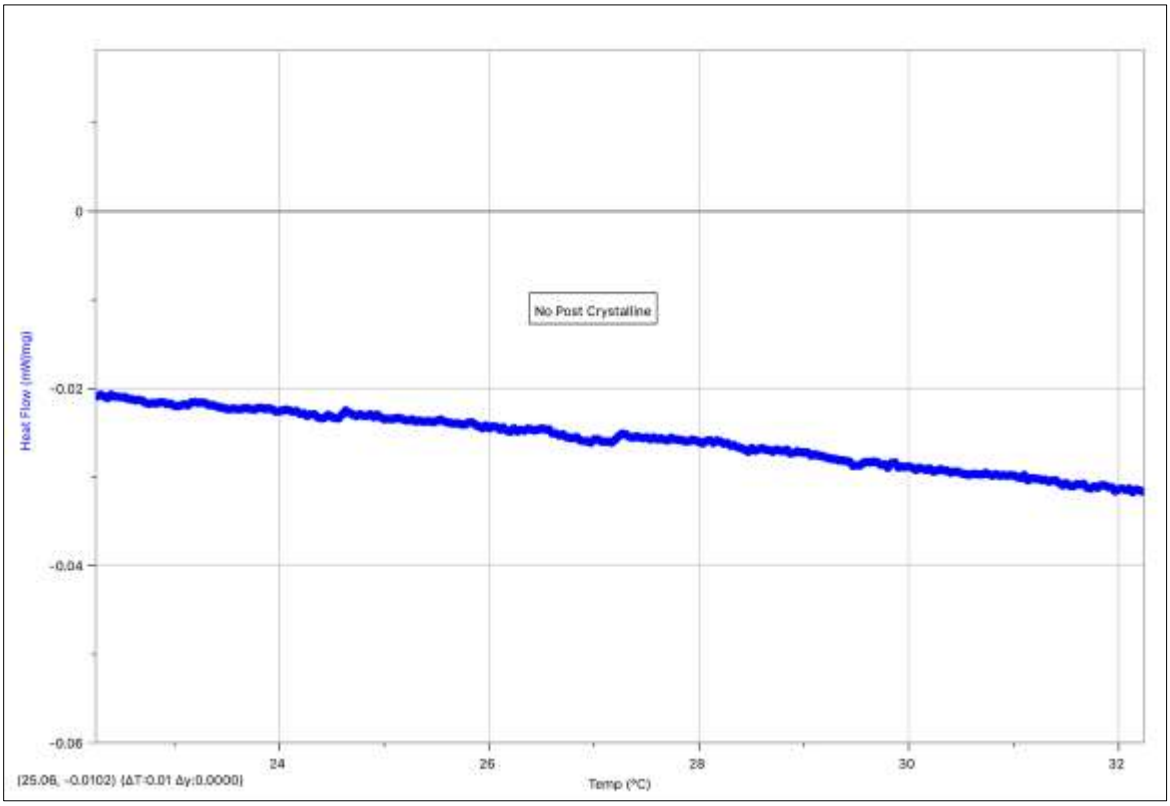

Fig. 46 Zoomed-in graph of Heat Flow (HF) vs Temperature (T) post-crystalline phase in 10OCB sample, in cooling.

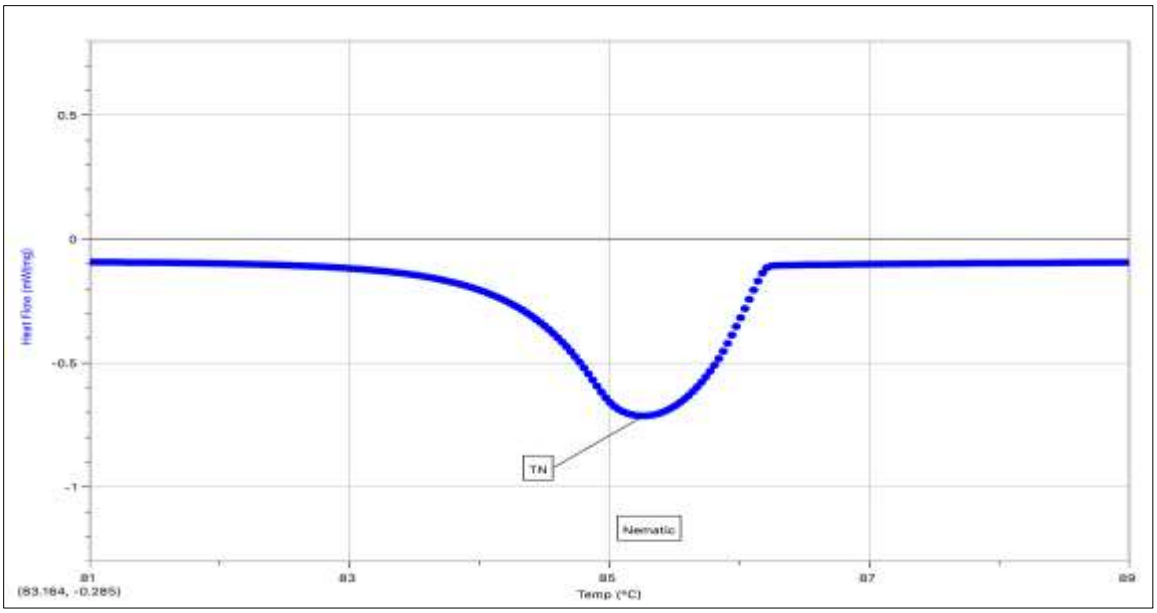

Fig. 47 Zoomed-in graph of Heat Flow (HF) vs Temperature (T) nematic phase in 10OCB sample, in cooling.

In Figures 45-47, zoomed-in images of all important peaks of phase change transitions of 10OCB found when analyzing the sample in cooling can be seen. Figure 45 highlights the crystalline phase, Figure 46 highlights that there is no post-crystalline phase, and Figure 47 highlights the nematic phase.

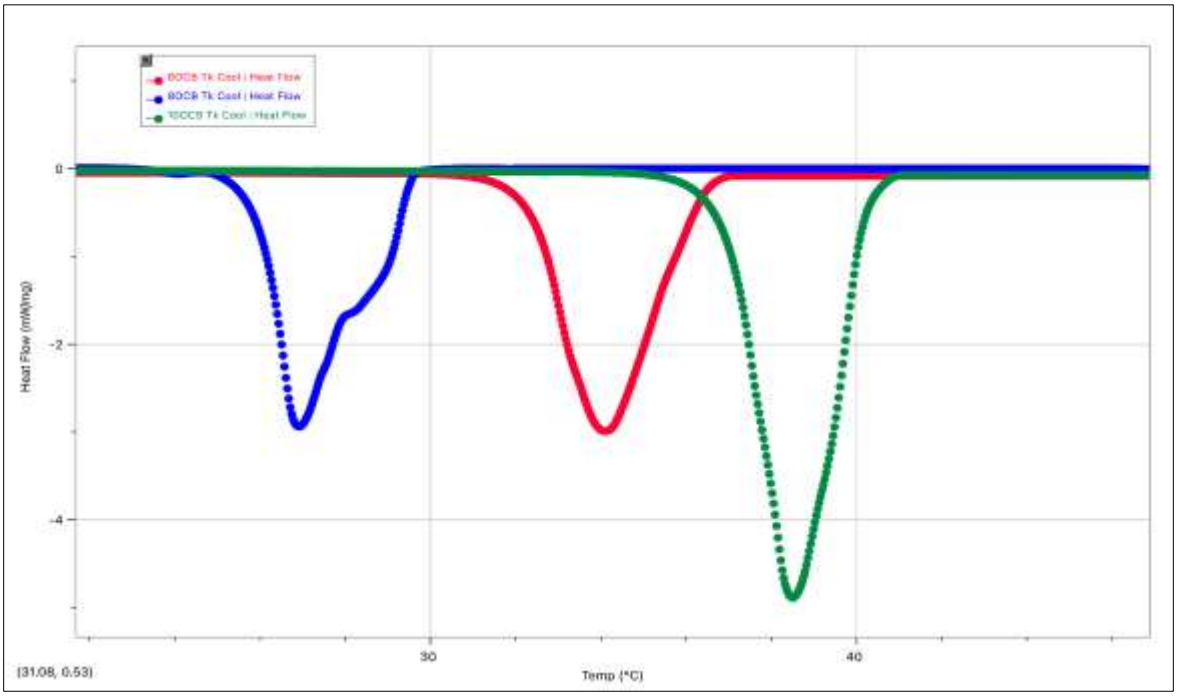

Fig. 48 Zoomed-in graph of Heat Flow (HF) vs Temperature (T) for crystalline phase for all three samples, 6OCB, 8OCB, and 10OCB, cooling only.

Seen above in Figure 48 is a comparison of the crystalline phase of all three samples during cooling. It can clearly be seen that 10OCB experiences the crystalline phase first, with a large, sharp peak, followed by the 6OCB with a shorter and wider peak, and finally the 8OCB with a short and wide double peak.

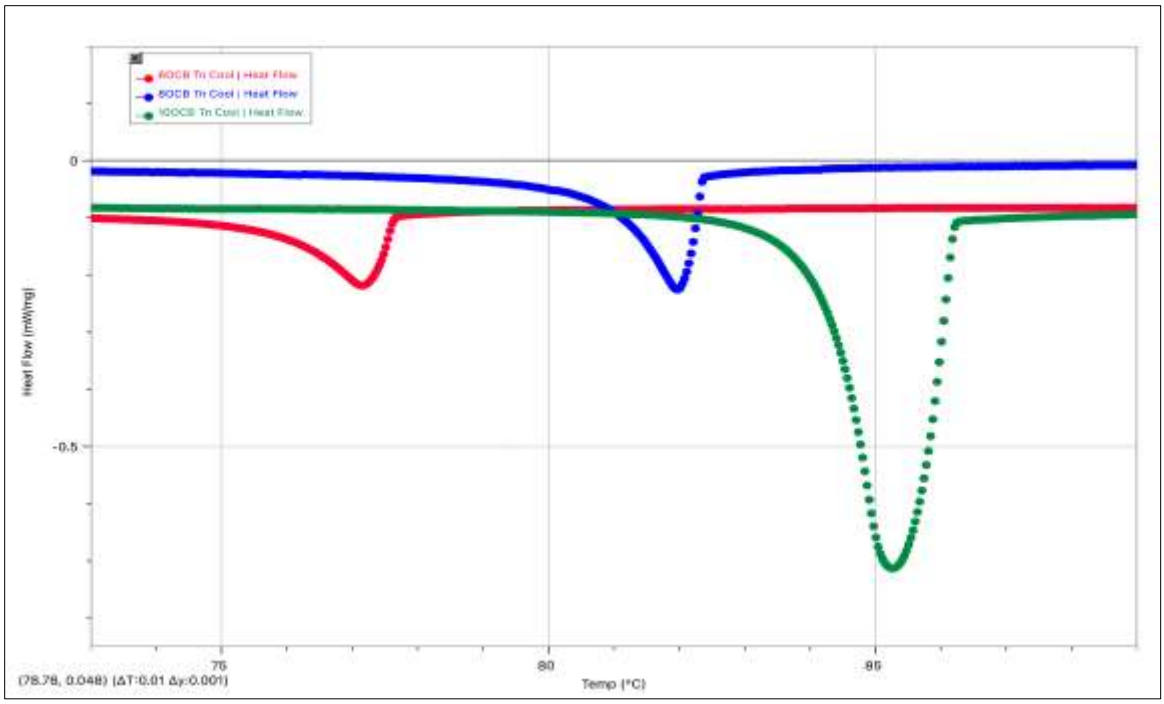

Fig. 49 Zoomed-in graph of Heat Flow (HF) vs Temperature (T) for the nematic phase for all three samples, 6OCB, 8OCB, and 10OCB, cooling only.

Comparison of nematic peaks for all three samples can be seen above in Figure 49, during cooling. It can be observed that 10OCB displays a large nematic peak first, followed by 8OCB with a small and narrow nematic peak, and finally 6OCB with a much shorter and narrower nematic peak.

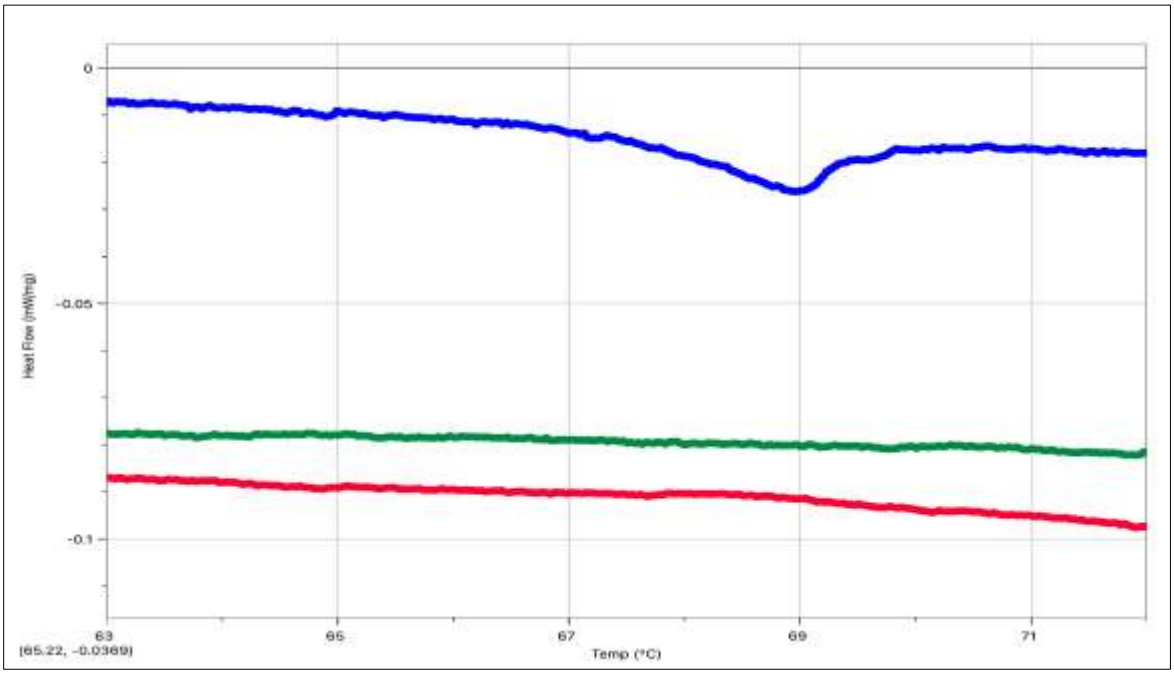

Fig. 50 Comparison of Smectic A in the 8OCB sample to no evidence of Smectic A in 6OCB and 10OCB samples, in cooling.

As seen above in Figure 50, the comparison of the smectic A phase in cooling, the only sample of the three to experience a smectic A phase is 8OCB. The 6OCB and 10OCB samples do not display a Smectic A phase when cooling.

2.6. Discussion

It is described above in the results section in detail how each sample shows its transitions in heating and cooling with a 5 °C/min ramp rate using DSC. It can be seen how the 6OCB and 10OCB behave in comparison to the 8OCB LC. To understand the uniqueness of 6OCB and 10OCB LCs, some summary graphs are plotted below to see significant results of each transition found in 6OCB and 10OCB compared with 8OCB, considering 8OCB as a typical member of the nOCB family with an Oxygen atom in the nOCB molecule. The 8OCB has been studied in detail by other authors, and these details can be seen in these publications. [15-19] The goal is to find how 6OCB and 10OCB behave differently from 8OCB. The 8OCB has an 8CH chain in the tail of its LC, whereas 6OCB has 6CH, and 10OCB has a 10CH chain in its tail. The nOCB molecule is a long molecule and hence takes the shape of a rod-like structure, including its chemical groups and CH tail. The difference in CH numbers in the tail brings significant differences in 6OCB and 10OCB LC compared to 8OCB. These changes can be seen in the summary plots shown below.

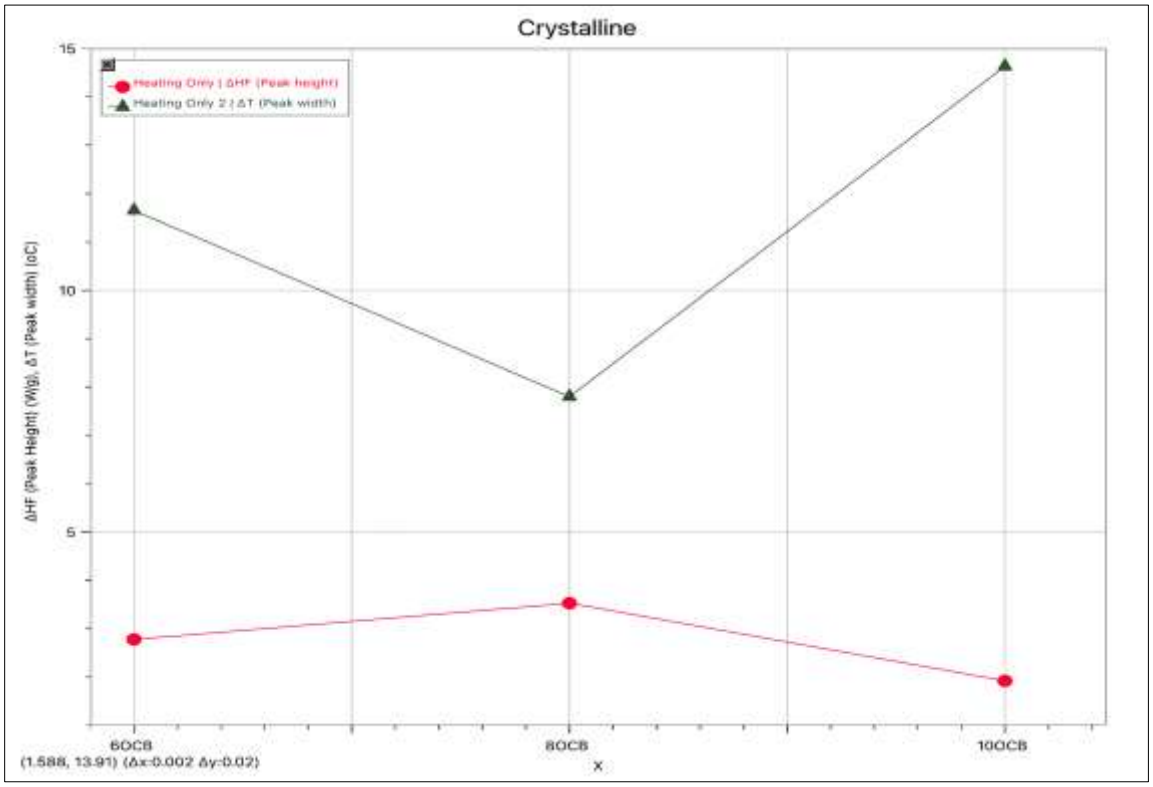

Fig. 51 Summary graph of 6OCB, 8OCB, and 10OCB showing ΔHF Peak Heights and ΔT Peak widths for heating only in the crystalline phase.

Peak heights and widths of the crystalline phase in heating of all three samples, showcased above in Figure 51, can be analyzed to point out the uniqueness of the behaviors of 6OCB and 10OCB in comparison to the typical member of the nOCB family, 8OCB. In the crystalline phase, the peak heights of both 6OCB and 10OCB are seen as being less than 8OCB, while the peak widths of 6OCB and 10OCB are seen as being more than 8OCB. This data indicated that 8OCB has the most well-ordered crystalline phase and is the most stable among the family, while 6OCB and 10OCB have much less ordered and therefore less stable crystalline states. Overall, it can be said that a taller and sharper crystalline peak indicates a more stable phase, while shorter and broader peaks indicate a more unstable phase.

Peak heights and widths of the crystalline phase in the cooling of all three samples, showcased in Figure 52, can be analyzed to again point out the uniqueness of the behaviors of 6OCB and 10OCB in comparison to 8OCB. In the crystalline phase, the peak height of 10OCB is seen to be much larger than both 8OCB and 6OCB, which are relatively similar. The peak widths in the crystalline phase show 6OCB and 10OCB as being much less than the peak width of 8OCB. It can be said that since 10OCB has the tallest and sharpest peak in crystalline cooling, this LC has the highest order.

Since 8OCB and 6OCB have similar, smaller peak heights, their crystal order is lower. Although 6OCB and 10OCB have narrow peak widths, with 8OCB having the widest peak width, indicating that 8OCB is the most disordered in cooling during the crystalline phase. Overall, 10OCB has the most ordered and stable crystalline phase, followed by 6OCB, and 8OCB has the least ordered and stable crystalline phase, all in cooling.

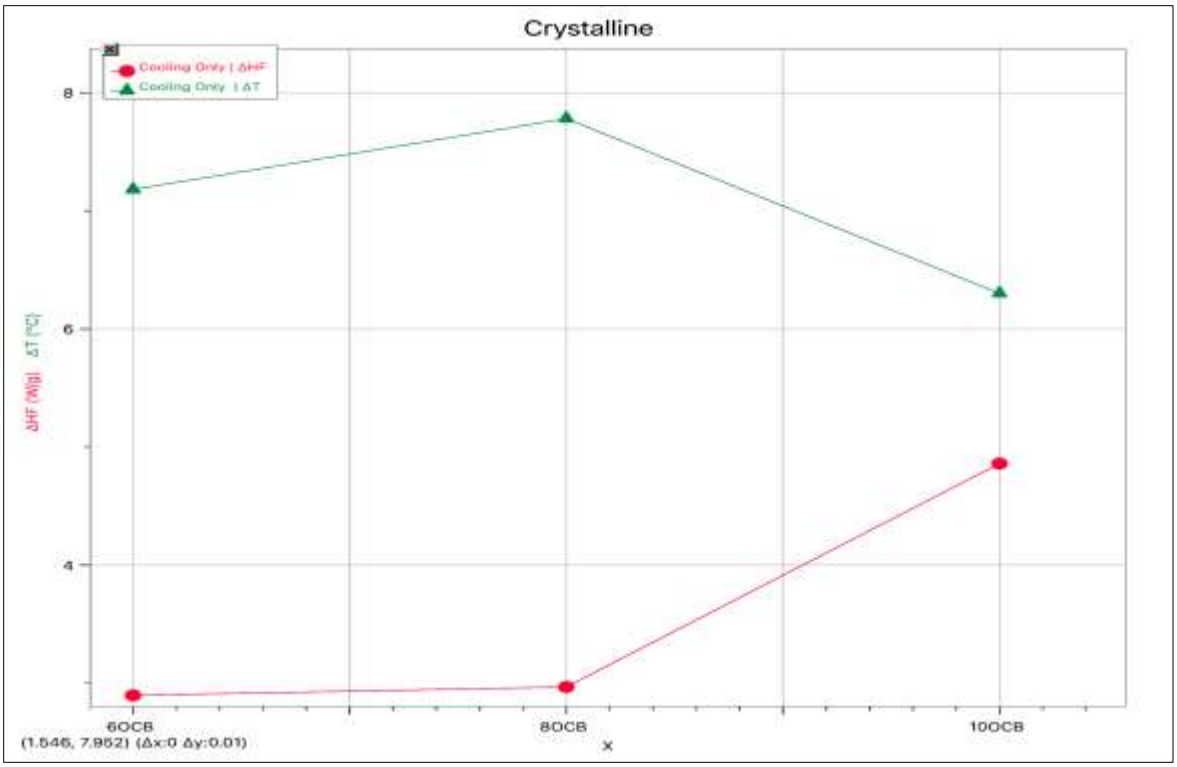

Fig. 52 Summary graph of 6OCB, 8OCB, and 10OCB ΔHF Peak Heights and ΔT Peak widths for cooling only in the crystalline phase.

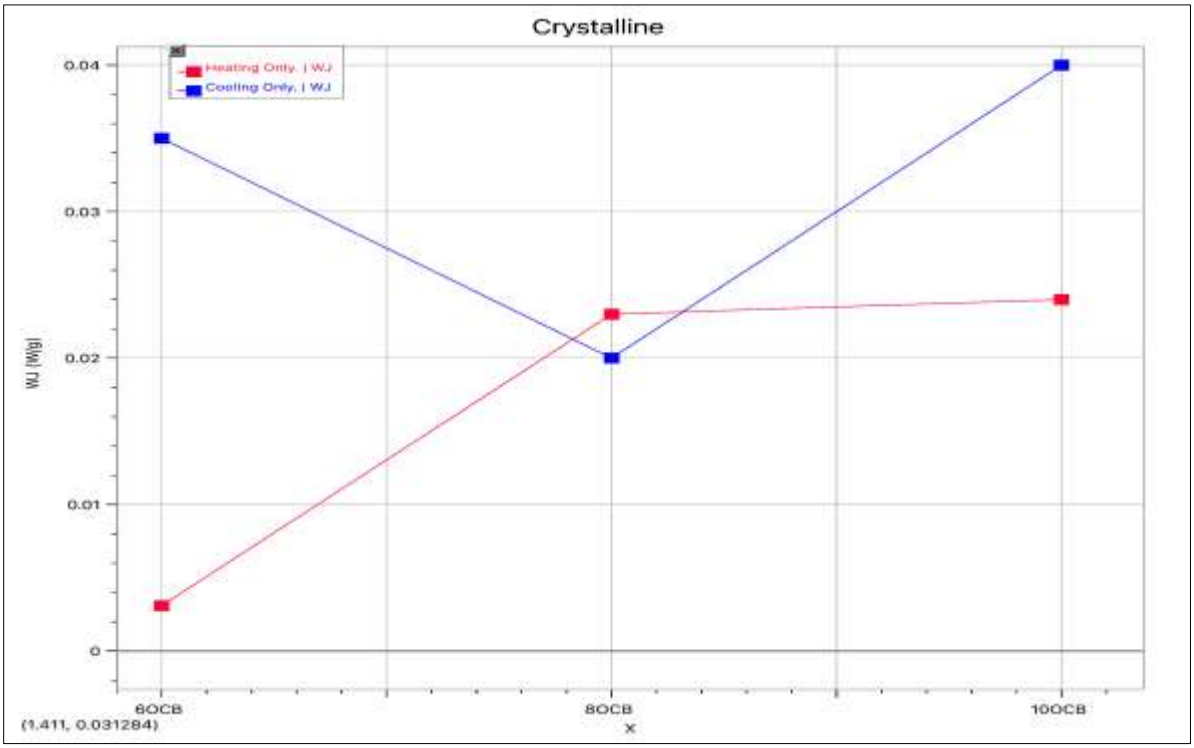

Fig. 53 Summary graph of 6OCB, 8OCB, and 10OCB Wing Jump (WJ) for both heating and cooling in the crystalline phase.

The wing jump for all 3 samples in the crystalline phase can be observed above in Figure 53, to examine the stability and dynamicness of the LCs. In heating, 6OCB shows the lowest wing jump value, with 8OCB and 10OCB showing relatively similar wing jump values. This data indicates that 6OCB needs less energy and less structural rearrangement to

leave the crystalline phase, while 8OCB and 10OCB, having similar values, require more energy and structural change to melt, and therefore are more stable during heating. In cooling, however, 6OCB and 10OCB show relatively similar and much higher wing jump values than 8OCB. The 6OCB and 10OCB samples, with similar wing jump values, undergo larger structural changes when cooling in the crystalline phase, indicating they form the crystal lattice more easily. [18] 8OCB, showing the lowest wing jump value in cooling, indicates it is more dynamic or less stable and more disordered.

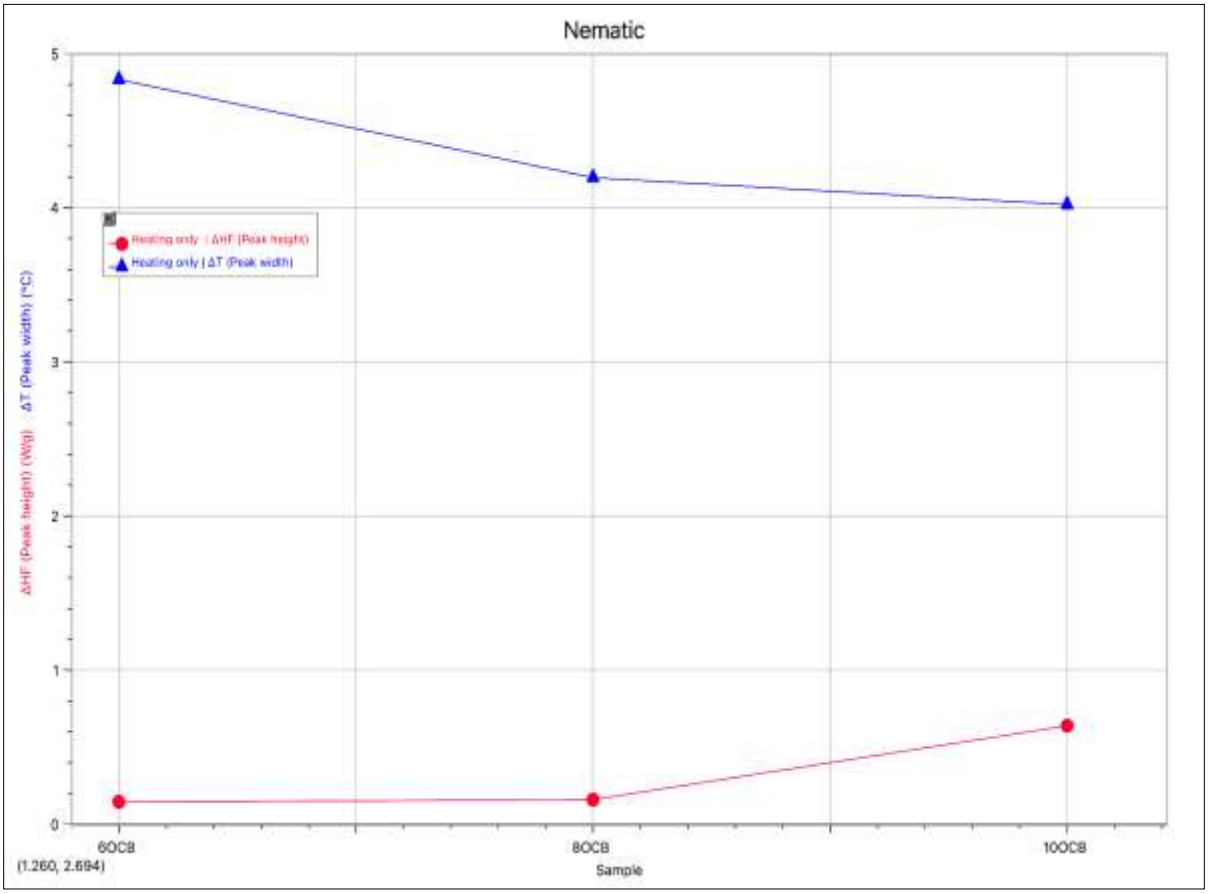

Fig. 54 Summary graph of 6OCB, 8OCB, and 10OCB ΔHF Peak Heights and ΔT Peak widths for heating only in the nematic phase.

Peak heights and widths of the nematic phase in heating of all three samples, showcased above in Figure 54, can be analyzed to point out the uniqueness of the behaviors of 6OCB and 10OCB in comparison to 8OCB again. In the nematic phase, the peak height of 10OCB is seen to be the largest, while 8OCB and 6OCB are smaller and relatively similar. The 6OCB nematic peak width is seen to be the largest, followed by 8OCB as an intermediate width, and 10OCB with the smallest peak width.

According to this data, 10OCB has the most ordered and stable nematic structure in comparison to 8OCB and 6OCB, indicating that a larger peak height and smaller peak width present the most ordered structure. 8OCB, being an intermediate in peak width, would indicate that this LC has moderate disorder. The 6OCB, having the smallest peak height with the largest peak width, indicates it has the least ordered and least stable nematic structure.

Peak heights and widths of the nematic phase in the cooling of all three samples, showcased above in Figure 55, can be analyzed to again point out the uniqueness of the behaviors of 6OCB and 10OCB in comparison to 8OCB. In the nematic phase, the peak height of 10OCB is seen to be much larger than both 8OCB and 6OCB, which are relatively similar. The peak widths in the nematic phase show 6OCB as being the largest, followed by 8OCB next, and 10OCB as being the smallest.

The 10OCB has the most stable nematic ordering due to its large peak height and small peak width, while 6OCB, with a smaller peak height and larger peak width, indicates that it is more disordered and the least stable sample in the nematic phase. The 8OCB shows moderate disorder due to its intermediate width and small height, in comparison to 6OCB and 10OCB.

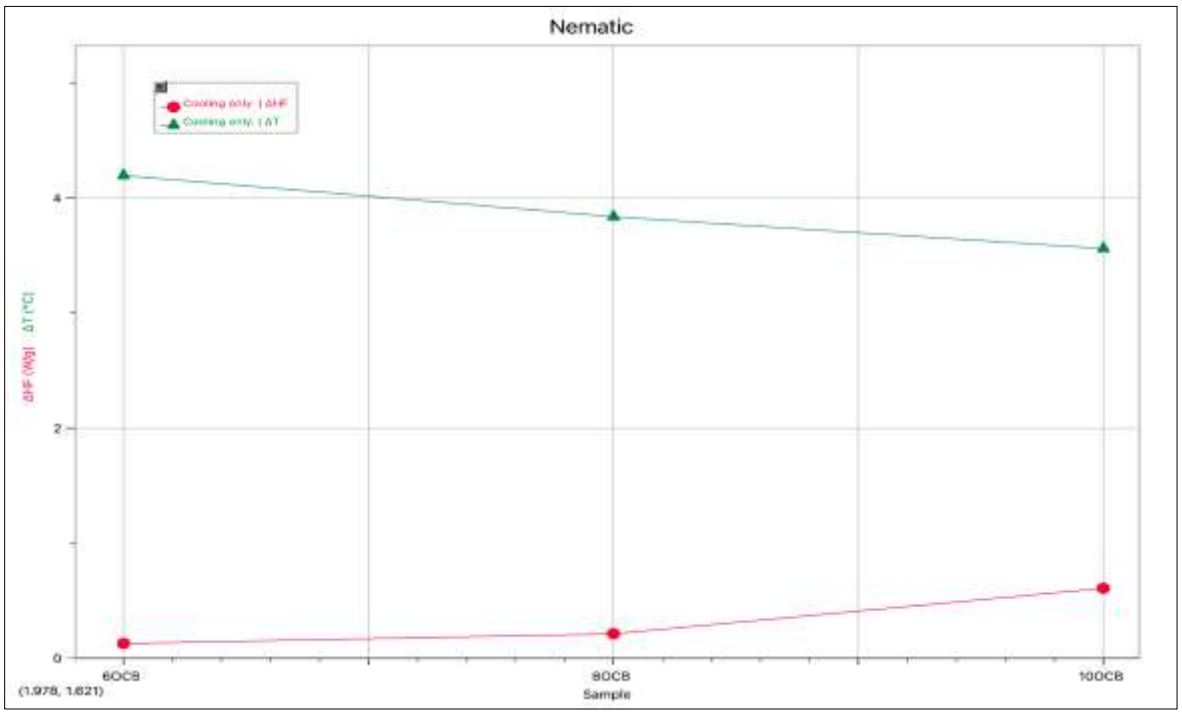

Fig. 55 Summary graph of 6OCB, 8OCB, and 10OCB ΔHF Peak Heights and ΔT Peak widths for cooling only in the nematic phase.

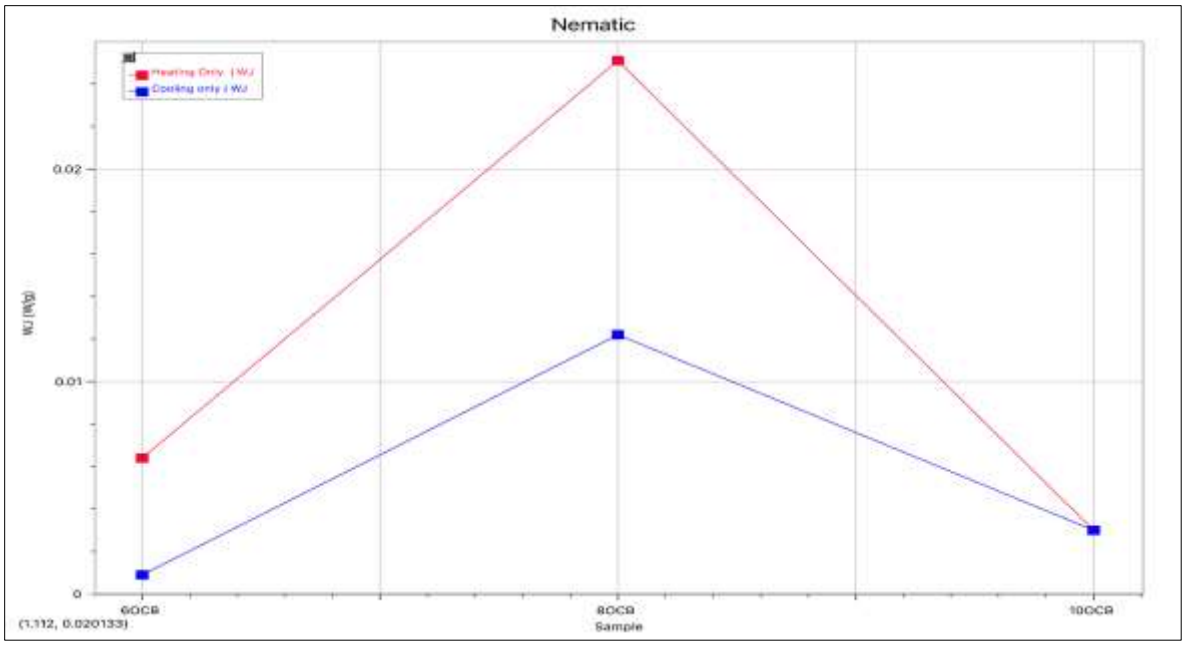

Fig. 56 Summary graph of 6OCB, 8OCB, and 10OCB Wing Jump (WJ) for both heating and cooling in the nematic phase.

The wing jump for all 3 samples in the nematic phase can be observed in Figure 56, to again examine the stability and dynamicness of the LCs. In both heating and cooling, 6OCB and 10OCB show very low wing jump values in comparison to 8OCB, which displays high wing jump values in both heating and cooling. The 6OCB and 10OCB LCs are behaving very similarly and are highly stable in the nematic phase, regarding the wing jump observed. These two LCs are seen to be very stable and undergo fewer structural changes. [18] The 8OCB LC showing the large wingjump values indicates that the LC is much less stable and more dynamic than the 6OCB and 10OCB in the nematic phase, meaning that it must undergo more structural rearrangement.

Table 5(a). Detail Analysis of Each Peak for Heating 6OCB.

Transition	Peak Height ΔHF (W/g)	Peak Width ΔT (°C)	Peak Jump WJ (W/g)
Tpre	0.003	7.42	0.0434
Tk	2.781	11.65	0.0031
Tpo			
Tsm			
Tn	0.146	4.831	0.0064

Table 5(b). Detail Analysis of Each Peak for Heating 8OCB.

Transition	Peak Height ΔHF (W/g)	Peak Width ΔT (°C)	Peak Jump WJ (W/g)
Tpre			
Tk	3.531	7.8	0.023
Tpo			
Tsm	0.0064	3.827	0.0049
Tn	0.1603	2.071	0.0251

Table 5(c). Detail Analysis of Each Peak for Heating 10OCB.

Transition	Peak Height ΔHF (W/g)	Peak Width ΔT (°C)	Peak Jump WJ (W/g)
Tpre			
Tk	1.925	14.62	0.024
Tpo	1.201	3.712	-1.439
Tsm			
Tn	0.64	4.02	0.003

Table 6(a). Detail Analysis of Each Peak for Cooling 6OCB.

Transition	Peak Height ΔHF (W/g)	Peak Width ΔT (°C)	Peak Jump WJ (W/g)
Tpre			
Tk	2.898	7.18	0.035
Tpo			
Tsm			
Tn	0.1255	4.195	0.0009

Table 6(b). Detail Analysis of Each Peak for Cooling 8OCB.

Transition	Peak Height ΔHF (W/g)	Peak Width ΔT (°C)	Peak Jump WJ (W/g)
Tpre			
Tk	2.969	7.78	0.02
Tpo			
Tsm	0.0601	6.55	0.0074
Tn	0.21	3.837	0.0122

Table 6(c). Detail Analysis of Each Peak for Cooling 10OCB.

Transition	Peak Height ΔHF (W/g)	Peak Width ΔT (°C)	Peak Jump WJ (W/g)
Tpre			
Tk	4.86	6.3	0.04
Tpo			
Tsm			
Tn	0.606	3.56	0.003

Table 7. Nematic Range of All Samples for Heating and Cooling.

	Nematic Range	Nematic Range
Sample	Heating (°C)	Cooling (°C)
6OCB	15.78	42.97
8OCB	23.501	55.04
10OCB	22.15	46.77

Above in Data Tables 5a-6c, the peak heights, peak widths, and wing jumps, in heating and cooling of all three samples, can be seen as a clearer interpretation of Figures 51-56.

Above in Data Table 7, the nematic ranges of all three samples in heating and cooling can be seen. 6OCB has the smallest nematic range, meaning that it transitions through this phase at lower temperatures and has a lower stability window. 10OCB is seen as having an intermediate nematic range and has moderate stability in the nematic phase. 8OCB has the widest nematic range of the three samples, meaning that it stays in the nematic phase over the largest temperature span and is the most thermally stable in this phase.

Table 8(a). Summary of Peak Values for Heating.

Sample	Peak height (N), W/g	Peak width (N), °C	TN, °C	Wing Jump (N), W/g	Peak height (K), W/g	Peak width (K), °C
6OCB	0.146	4.831	78.74	0.0064	2.781	11.65
8OCB	0.1603	2.071	83.14	0.0251	3.531	7.8
10OCB	0.64	4.02	87.76	0.003	1.925	14.62

Table 8(b). Summary of Peak Values for Cooling.

Sample	Peak height (N), W/g	Peak width (N), °C	TN, °C	Wing Jump (N), W/g	Peak height (K), W/g	Peak width (K), °C
6OCB	0.1255	4.195	77.19	0.0009	2.898	7.18
8OCB	0.21	3.837	82.02	0.0122	2.969	7.78
10OCB	0.606	3.56	85.29	0.003	4.86	6.3

As reflected above in Data Tables 8a and 8b, the summaries of the peak values for heating and cooling of all three LCs are provided. Overall, 6OCB is seen to have the lowest TN, the smallest peak heights, but is stable in the nematic phase with a low wing jump. 10OCB is seen to display the strongest peak transitions, the highest TN, and stability of a low wing jump, but has broad transitions. 8OCB has the sharpest nematic transitions, with an intermediate TN, but is the least stable LC with the highest wing jump values.

Table 9(a). Summary of Total energy for heating and cooling combined.

Sample	Heating and Cooling Total energy (W/g*°C)
6OCB	43.72
8OCB	39.38
10OCB	48.12

Table 9(b). Summary of thermal energy for heating.

Sample	Total energy (W/g*°C)	PreK + K (W/g*°C)	K (W/g*°C)	K + PostK (W/g*°C)	SmA (W/g*°C)	N (W/g*°C)
6OCB	23.52	13.92	12.25			2.013
8OCB	25.08		11.01		1.057	2.093
10OCB	27.86		11.42	15.14		2.979

Table 9(c). Summary of thermal energy for cooling.

Sample	Total energy (W/g*°C)	K (W/g*°C)	SmA (W/g*°C)	N (W/g*°C)
6OCB	12.87	7.999		0.9929
8OCB	7.176	6.443	0.2131	0.4183
10OCB	16.12	10.52		1.561

Above, seen in Data Tables 9a-9c, are the thermal energies for heating and cooling of all three LC samples. Thermal energy indicates how much heat is needed for the sample to undergo a phase change. A higher thermal energy means that the phase change transition is stronger and more energetically demanding, while a lower thermal energy means that the transition is much weaker. In the data tables above, it can be noticed that 10OCB consistently requires the most total energy during both heating and cooling, meaning that its phase change transitions are the strongest and most energetically intense. 6OCB requires a moderate amount of energy to undergo phase change transitions. 8OCB consistently shows the lowest total energy to undergo phase change transitions, indicating that its phase change transitions are the weakest.

2.7. Predicted Model

To explain Pre-Crystalline in 6OCB and Post-Crystalline in 10OCB, this model is predicted.

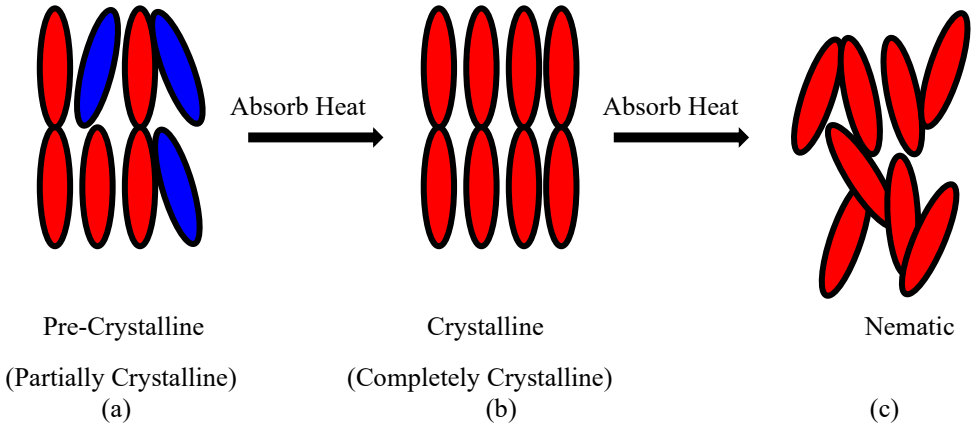

Fig. 57 Predicted model of 6OCB to explain the Pre-Crystalline state. The blue color represents the disordered molecules.

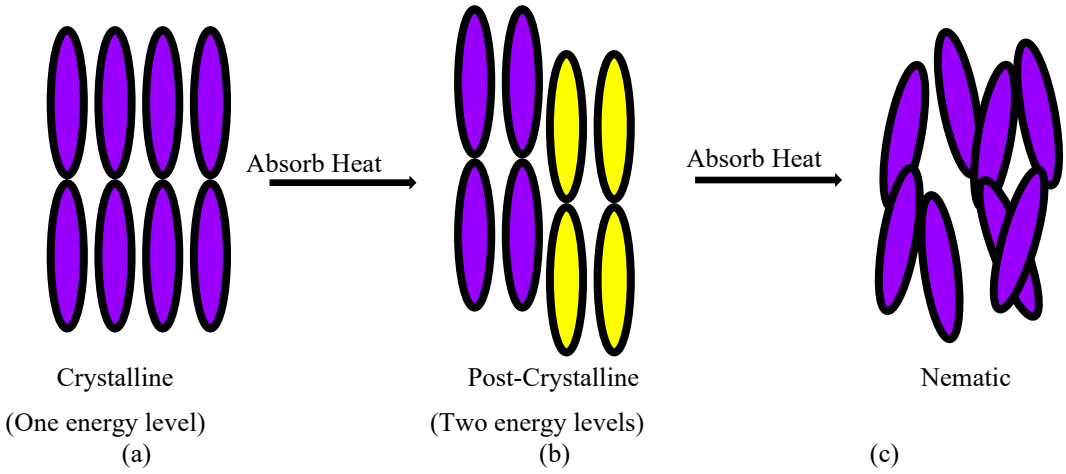

Fig. 58 Predicted model of 10OCB to explain the Post-Crystalline state. In part (b), purple and yellow show two energy levels

Shown in Figures 57 and 58 are the predicted molecular arrangements of the 6OCB and 10OCB LCs. In Figure 57, the Pre-Crystalline phase of the 6OCB LC is seen to obtain the same rows and columns seen in the Crystalline phase, but a few molecules have changed their directionality. In Figure 58, the Post-Crystalline phase of the 10OCB LC is also seen to

obtain the same columns and directionality as the Crystalline phase, but it no longer holds the rows. It can be seen that the rows in the Post-Crystalline phase seem to shift, and offset them slightly. More details regarding the behaviors of LC within the nOCB family can be seen here [19-22]. An example using DSC and Logger Pro can be seen in this publication. [23]

3. Conclusion

This research reports the novelty of the states that appeared in 6OCB and 10OCB LCs, which were not previously reported anywhere in the literature so far. This novelty makes this research important in the research area of LCs and their applications. Three samples of nOCB (6OCB, 8OCB, 10OCB) LCs were studied using the Differential Scanning Calorimetric technique with a 5 °C/min ramp rate for heating and cooling. Data was collected as heat flow versus temperature and time plots for them. Later, the specific heat capacity was calculated for them. The details of heat flow, thermal energy, specific heat capacity, types of transitions, and details of transitions that occurred in them were studied. It is found that 6OCB and 10OCB show some unique behavior that 8OCB does not show. The 6OCB is the smallest member of nOCB with a 6 CH chain in its tail, whereas 10OCB has a 10 CH chain in its tail. Based on the tail size, they show some unique transitions and states when they are heated. The 6OCB shows a unique state of precrystalline in heating, whereas 10OCB shows a unique state of post-crystalline in heating, when compared with 8OCB LC. These two new states bring the crystallization phase wider and take a longer time to occur when heated and cooled. These LCs show Nematic and Isotropic states as well. The Nematic is found much bigger in 10OCB. The 10OCB absorbs more thermal energy and shows stability in its transitions, whereas 6OCB shows longer time stability. A model is predicted to explain the behavior of 6OCB and 10OCB. The 6OCB is explained on the basis of the existence of a partially crystalline state, as the Pre-Crystalline state in 6OCB, as it has the smallest tail size. At the same time, 10OCB is explained based on two energy levels as Crystalline and Post-Crystalline states, as it has the longest tail in its molecule. The increased stability of 6OCB and 10OCB can be used in Liquid Crystal Display devices (LCDs), smart devices, and medical sciences, where LCs are used.

Overall, it can be concluded that 10OCB has the highest nematic peaks, in heating being 0.64 W/g and in cooling being 0.606 W/g, while the 6OCB LC shows the widest nematic peaks, in heating being a range of 4.83°C and in cooling being a range of 4.20°C. In heating, the nematic peak for 6OCB occurs first at 78.74°C, and the 10OCB nematic peak occurs last at 87.76°C, with 8OCB being an intermediate at 83.14°C. We can see this same pattern in cooling as well, with the 6OCB nematic peak being displayed first at 77.19°C, and the 10OCB nematic peak last at 85.29°C, with 8OCB, again, being an intermediate at 82.02°C. The 6OCB and 10OCB LCs have the smallest, almost negligible wing jump values in the nematic peaks, while 8OCB shows a wing jump of 0.0251 W/g in heating and 0.0122 W/g in cooling. In heating during the crystallization phase, 6OCB and 10OCB show larger peak widths than 8OCB, but in cooling, there is not much difference in crystalline peak widths, due to the absence of the pre and post-crystalline phases in cooling, for 6OCB and 10OCB, respectively. In the summary of thermal energy, it can be concluded that 10OCB takes in the greatest amount of energy in both heating, and 6OCB takes in the least amount of energy in heating, with 8OCB, again, being an intermediate.

Acknowledgement

The authors are thankful to Professor John C. MacDonald from the Chemistry and Biochemistry department and Life Sciences and Bioengineering Center, WPI, Worcester, MA, for providing the DSC model NETZSCH 214 instrument. Authors are also thankful to the NETZSCH company for providing the DSC 214 pans and lids. The student author likes to acknowledge Dr. Dipti Sharma for supervising this research internship with Liquid Crystal and Emmanuel College for running internship programs.

References

[1] Jeff Tyson, How LCDs Work, HowStuffWorks. [Online]. Available: https://electronics.howstuffworks.com/lcd.htm

[2] Mathew C. Doran, Medaelle Seide, and Dipti Sharma, "Reporting Strange and Unique Behavior of 4CB Liquid Crystal using Logger Pro," *International Journal of Research in Engineering and Science (IJRES)*, vol. 10, no. 5, pp. 27-41, 2022. [Publisher Link]

[3] Dipti Sharma, "Non-isothermal Kinetics of Melting and Nematic to Isotropic Phase Transitions of 5CB Liquid Crystal," *Journal of Thermal Analysis and Calorimetry*, vol. 102, no. 2, pp. 627–632, 2010. [CrossRef] [Google Scholar] [Publisher Link]

[4] Materials Science and Engineering: Liquid Crystals, Department of Materials Science and Engineering. [Online]. Available: https://mse.umd.edu/about/what-is-mse/liquid-crystals

[5] What is a liquid crystal display (Lcd)?, Lenovo. [Online]. Available: https://www.lenovo.com/ca/en/glossary/what-is-lcd/

[6] Mohamed B. Sied et al., "Binary Mixtures of nCB and nOCB Liquid Crystals. Two Experimental Evidences for a Smectic A–Nematic Tricritical Point," *Physical Chemistry Chemical Physics*, no. 12, 2002. [CrossRef] [Google Scholar] [Publisher Link]

[7] Dipti Sharma, "Non-Isothermal Kinetics of Melting and Nematic to Isotropic Phase Transitions of 5CB Liquid Crystal," Journal of Thermal Analysis and Calorimetry, vol. 102, no. 2, pp. 627-632, 2010.[CrossRef] [Google Scholar] [Publisher Link]

[8] Kris McDonough, Ngoc Chau Vy, and Dipti Sharma, "Existence of Time Lag in Crystalline to Smectic A (K–SmA) Phase Transition of 4-decyl-4-Biphenylcarbonitrile (10CB) Liquid Crystal," *Journal of Thermal Analysis and Calorimetry*, vol. 116, pp. 1515–1520, 2014. [CrossRef] [Google Scholar] [Publisher Link]

[9] William LeBrun, and Dipti Sharma, "Characterizing Mesophase Transitions of 8CB Liquid Crystal using DSC and Logger Pro," *Engineering and Technology Journal*, vol. 9, no. 7, 2024. [CrossRef] [Publisher Link]

[10] G. Petrarca, "Reporting Kinetics and Dynamics of Phase Transitions of 8OCB Liquid Crystal using Logger Pro," *International Journal of Research in Engineering and Science (IJRES)*, vol. 13, no. 4, pp. 69–88, 2025. [Publisher Link]

[11] Grace Petrarca, and Dipti Sharma, "Isothermal and Non-Isothermal Study of 8OCB Liquid Crystal using DSC and Logger Pro," *Engineering and Technology Journal*, vol. 9, no. 7, 2024. [CrossRef] [Publisher Link]

[12] Grace Petrarca, and Dipti Sharma, "Presenting Percent Crystallinity and Crystallization Order of 8OCB Liquid Crystal," *International Journal of Applied Physics*, vol. 12, no. 2, pp. 1-11, 2025. [CrossRef] [Publisher Link]

[13] Han Fei, "The Importance and Applications of Heat Capacity: Investigating a Fundamental Property of Matter," *Journal of Thermodynamics and Catalysis,* vol. 14, no. 3, 2023. [CrossRef] [Publisher Link]

[14] Dipti Sharma, John C. MacDonald, and Germano S. Iannacchione, "Role of Aerosil Dispersion on the Activated Kinetics of the $LC_{1-x}Sil_x$ System," *The Journal of Physical Chemistry B,* vol. 110, no. 51, pp. 26160–26169, 2006. [CrossRef] [Google Scholar] [Publisher Link]

[15] Dipti Sharma, "Kinetics of Nanocolloids in the Aligned Domain of Octylcyanobiphenyl and Aerosil Dispersion," *Liquid Crystals,* vol. 35, no. 10, pp. 1215–1224, 2008. [CrossRef] [Google Scholar] [Publisher Link]

[16] D. Sharma, "Calorimetric Study of Activated Kinetics of the Nematic and Smectic Phase Transitions in an Aligned Nano-Colloidal Liquid Crystal + Aerosil Gel," *Journal of Thermal Analysis and Calorimetry,* vol. 93, pp. 899–906, 2008. [CrossRef] [Google Scholar] [Publisher Link]

[17] Dipti Sharma, "The Effect of Alignment on the Nematic to Isotropic Phase Transition of Bulk Octylcyanobiphenyl Brings Possible Solutions to Liquid Crystal Displays," *Applied Physics Letters,* vol. 94, no. 13, 2009. [CrossRef] [Google Scholar] [Publisher Link]

[18] Medaelle Seide, and Dipti Sharma, "Reporting Phase Transitions of a New Generation "Tertiary Liquid Crystal System" (TLCS) using Logger Pro," *SSRG International Journal of Applied Physics*, vol. 10, no. 1, pp. 22–33, 2023. [CrossRef] [Google Scholar] [Publisher Link]

[19] Laura Elizabeth Byrne, and Dipti Sharma, "Effect of Heating and Cooling on 6CB Liquid Crystal Using DSC Technique," *Engineering and Technology Journal*, vol. 8, no. 9, pp. 2740–2756, 2023. [CrossRef] [Publisher Link]

[20] Medaelle Seide, Mathew C. Doran, and D. Sharma, "Analyzing Nematic to Isotropic (N-I) Phase Transition of NCB Liquid Crystals using Logger Pro," *European Journal of Applied Sciences*, vol. 10, no. 3, 2022. [CrossRef] [Google Scholar] [Publisher Link]

[21] Juliana Mello, and Dipti Sharma, "Details of Nematic Phase Transition and Nematic Range of 5OCB Liquid Crystal using Logger Pro," *International Journal of Research in Engineering and Science (IJRES)*, vol. 10, no. 9, pp. 197–217, 2022. [Google Scholar]

[22] Juliana Mello, and Dipti Sharma, "Crystal Growth, Percent Crystallinity and Degree of Crystallization of 5OCB Liquid Crystal (Analyzing using Logger Pro)," *International Journal of Engineering Inventions*, vol. 12, no. 1, pp. 166-185, 2023. [Publisher Link]

[23] Melanie Phares, and Dipti Sharma, "Analyzing and Reporting the Physics of Chewing Gum and Its Impact on Dental Health Using Differential Scanning Calorimetry (DSC) and Logger Pro," *Journal of Dental and Oral Research*, vol. 6, no. 3, pp. 1–18, 2025. [CrossRef] [Google Scholar] [Publisher Link]